Geomorphology
February 2018, Volume 303 Pages 338-356
https://doi.org/10.1016/j.geomorph.2017.11.021
https://archimer.ifremer.fr/doc/00638/74997/

Neogene-Quaternary slow coastal uplift of Western Europe through the perspective of sequences of strandlines from the Cotentin Peninsula (Normandy, France)

Pedoja K. [1, 2, 3, *], Jara-Munoz J. [4], De Gelder G. [5], Robertson J. [6], Meschis M. [6], Fernandez-Blanco D. [5], Nexer Maelle [1, 2, 3], Poprawski Y. [7], Dugue O. [1, 2, 3], Delcaillau B. [1, 2, 3], Bessin P. [8], Benabdelouahed M. [9, 10], Authemayou C. [9, 10], Husson L. [11, 12, 13], Regard V. [14, 15, 16], Menier D. [9, 10], Pinel B. [1, 2, 3]

[1] Normandie Univ, Caen, France.
[2] UCBN, M2C, F-14000 Caen, France.
[3] CNRS, UMR M2C 6143, F-14000 Caen, France.
[4] Univ Potsdam, Inst Erd & Umweltwissensch, D-14476 Potsdam, Germany.
[5] Univ Paris Diderot, UMR CNRS 7154, Inst Phys Globe Paris, Sorbonne Paris Cite, F-75005 Paris, France.
[6] Birkbeck Univ London, Dept Earth & Planetary Sci, London WC1E 7HX, England.
[7] ICTJA CSIC, Inst Earth Sci Jaume Almera, Grp Dynam Lithosphere, Barcelona, Spain.
[8] Univ Maine, LPG Le Mans, UMR 6112, Ave Olivier Messiaen, F-72085 Le Mans, France.
[9] Univ Brest, CNRS, Lab Domaines Ocean, UMR IUEM 6538, Plouzane, France.
[10] Univ Bretagne Sud, GMGL IUEM CNRS Domaines Ocean 6538, Lorient, France.
[11] Univ Grenoble Alpes, ISTerre, F-38014 Grenoble, France.
[12] CNRS, ISTerre, F-38014 Grenoble, France.
[13] IRD, ISTerre, F-38014 Grenoble, France.
[14] Univ Toulouse, UPS OMP, GET, 14 Av Edouard Belin, F-31400 Toulouse, France.
[15] CNRS, GET, F-31400 Toulouse, France.
[16] IRD, GET, F-31400 Toulouse, France.

* Corresponding author : K. Pedoja, email address : kevin.pedoja@unicaen.fr

Abstract :

The Cotentin Peninsula (Normandy, France) displays sequences of marine terraces and rasas, the latter being wide Late Cenozoic coastal erosion surfaces, that are typical of Western European coasts in Portugal, Spain, France and southern England. Remote sensing imagery and field mapping enabled reappraisal of the Cotentin coastal sequences. From bottom to top, the N Cotentin sequence includes four previously recognized Pleistocene marine terraces (T1 to T4) at elevations <40 m as well as four higher and older rasas (R1 to R4) reaching 200 +/- 5 m in elevation. Low-standing marine terraces are not observed in the central part of the Peninsula and a limited number of terraces are described to the south. The high-standing rasas are widespread all over the peninsula. Such strandline distributions reveal major changes during the Late Cenozoic. Progressive uplift of an irregular sea-floor led to subaerial exposure of bathymetric highs that were carved into rocky platforms, rasas and marine terraces.

Eventually, five main islands coalesced and connected to the mainland to the south to form the Cotentin Peninsula. On the basis of previous dating of the last interglacial maximum terrace (i.e. Marine Isotopic Stage, MIS 5e), sequential morphostratigraphy and modelling, we have reappraised uplift rates and derived: (i) mean Upper Pleistocene (i.e. since MIS 5e similar to 122 +/- 6 ka, i.e. kilo annum) apparent uplift rates of 0.04 +/- 0.01 mm/yr, (ii) mean Middle Pleistocene eustasy-corrected uplift rates of 0.09 +/- 0.03 mm/yr, and (iii) low mean Pleistocene uplift rates of 0.01 mm/yr. Extrapolations of these slow rates combined with geological evidence implies that the formation of the sequences from the Cotentin Peninsula occurred between 3 Ma (Pliocene) and 15 Ma (Miocene), which cannot be narrowed down further without additional research. Along the coasts of Western Europe, sequences of marine terraces and rasas are widespread (169 preserve the MIS Se benchmark). In Spain, Portugal, S England and other parts of western France, the sequences morphostratigraphy is very similar to that of Cotentin. The onset of such Western European sequences occurred during the Miocene (e.g. Spain) or Pliocene (e.g. Portugal). We interpret this Neogene-Quaternary coastal uplift as a symptom of the increasing lithospheric compression that accompanies Cenozoic orogenies.

Highlights

► Morpho-stratigraphy of low-lying terraces from N Cotentin ► Description of the polygenic coastal erosion surfaces (rasas) of Cotentin ► Late Cenozoic paleogeographic evolution ► Database on Neogene and Quaternary shorelines of Western Europe ► Wholesale analysis of the Late Cenozoic uplift of Western European coastlines

Keywords : Marine terrace, Rasa, Cotentin and Western Europe, Neogene and Quaternary coastal uplift

1 Introduction

Emerged sequences of fossil coastal landforms (marine terraces and rasas which are wide Late Cenozoic polygenic coastal platforms) with associated deposits ("raised beaches") are present along the shores of Western Europe, in Portugal, Spain, France, UK and Ireland (Pedoja et al., 2011; 2014). In France and in the British Isles, earlier studies (e.g., Prestwich, 1862-1863, 1892; Home, 1912; Coutard et al., 2006) - with notable exceptions (e.g., Guilcher 1974; Lautridou, 1989) - ignored the higher and older landforms (i.e. the rasas) within the coastal sequences, while in Iberia, rasas were long interpreted as geomorphic indicators of former sea levels (e.g., Breuil et al., 1942; Teixeira, 1944).

Herein, we reappraise the coastal sequences of the Cotentin Peninsula (Normandy, France) because this area exhibits some of the northernmost long-lasting (i.e. including rasa) coastal sequences along the Atlantic passive margin where Pleistocene coastal deformation is generally homogeneous over long distances (Pedoja et al., 2014). We mapped the Neogene and Quaternary strandlines from Cotentin and measured their elevations through field studies, satellite images (*Landsat*, *SPOT*) and Digital Elevation models DEM (MNT *Litto 3D* provided by *IGN,* Institut de Géographie National). Age controls come from previous studies at the same sites (e.g., Antoine et al., 1998; Cliquet et al., 2003; 2009; Coutard, 2003; Coutard et al., 2005, 2006, Clet-Pellerin et al., 1997; van Vliet-Lanoë et al., 2002; Dugué, 2003). We derived and extrapolated different Pleistocene uplift rates and undertook modelling to propose plausible age ranges for the undated strandlines of the sequence. The inferred timing is then discussed within the broader framework of regional geology. The Late Cenozoic paleogeographical evolution of Cotentin has already been interpreted as that of an island that connected to the mainland (see van Vliet-Lanoë et al., 2000; 2002). We present geomorphic evidence – the pattern of fossil shorelines associated with the rasas – which support this evolution.

In order to reframe the uplift of the Cotentin Peninsula and to evidence coastal uplift at a continental scale, we compiled a regional synthesis of Late Cenozoic sea-level changes for Atlantic Europe (Portugal, Spain, France, and the British Isles). The coastal sequences of Western Europe have been somehow neglected in the most recent global approaches (e.g. Murray-Wallace and Woodroffe, 2014; Pedoja et al., 2014) and not interpreted as a continuous, 2000 -km-long uplifted coastal segment.

2 Settings

2.1 Geodynamics and geology

Since the upper Cretaceous, the convergence between the African and the European plates affected the Western European passive margin. During the Pyrenees and the Alpine orogenies, the main compressive stages reactivated structures of the passive margin from upper Cretaceous to lower Miocene (e.g., Dèzes et al., 2004) with high convergence rates, (~ 20 mm/yr) during the upper Cretaceous (Rosenbaum et al., 2002). From the Late Miocene to the Quaternary, the convergence is characterized by low rates with a modern rate ranging from 2 to 5 mm/yr (Dèzes et al., 2004). In the foreland, convergence coincided with oblique extensional processes such as the opening of the European Cenozoic rifts (Dèzes et al., 2004).

The Cotentin Peninsula on the North Atlantic margin, forms a promontory into the English Channel (Fig. 1). The Peninsula belongs to the Armorican Massif and bounds the Paris Basin (Juignet, 1980). Its basement, into which the marine terraces and rasas are carved, is made of sedimentary and igneous rocks (Dupret et al., 1990; Ziegler and Dèzes, 2007; Ballèvre et al., 2009). Cadomian and Variscan faults delimit N 70° and N 120° grabens on the peninsula (Gresselin, 2000; Butaeye, 2001; Lagarde et al. 2000; 2003). During the second half of the Mesozoic, the Peninsula emerged and continental erosion/subtropical alteration induced the planation of the Variscan topography (Klein, 1975), although Cenomanian marine incursions are known (Dugué et al., 2007; 2009; Bessin, 2015). During the Cenozoic, compressive events alternated with relaxation phases (van Vliet-Lanoë et al., 2002); the Peninsula was exposed to alternating marine sedimentation (coming from the west) and continentalisation (Guilcher, 1949; Klein, 1975; Baize, 1998; Bonnet et al., 2000; van Vliet-Lanoë et al., 2002; Guillocheau et al., 2003; Dugué et al., 2007, 2009; Bessin et al., 2015). On the NW Armorican massif, Paleogene long wavelength/low amplitude deformation (Dugué, 2003; Dugué et al. 2007, 2009) resulted in uplift, emergence, and subtropical subaerial weathering of the area which led to the formation of a planation surface (Baize, 1998; Ziegler, and Dèzes, 2007). During the late Middle Eocene, the North Atlantic waters reoccupied the area (Dugué, 2003; Dugué et al., 2007, 2009; Bauer et al., 2016). Upper Eocene and Lower Oligocene deformations of the area (Bonnet et al., 2000; Guillocheau et al., 2003; Dugué, 2003; Dugué et al., 2007; 2009) induced a resurfacing of the main planation surface to a lower one.

North Cotentin emerged during the Upper Paleocene (Dugué et al., 2009), whereas in the Seuil du Cotentin basin (Fig. 1C), marine incursions occurred during the Oligocene and Middle Miocene times (Langhian – Serravallian, open marine facies; Baize, 1998; van Vliet-Lanoë et al., 2002; Dugué et al., 2009). As the closure of the seaway once constituted by the Seuil du Cotentin area is an important benchmark for the regional coastal evolution, its Plio-Quaternary sedimentary record is presented and discussed section 4.4.3.

2.2 Geomorphology

The English Channel bordering the Cotentin Peninsula is an epi-continental sea; its floor, presently at <60 m, emerged periodically over glacial cycle timescales. During low-stands, the sea bottom was dissected by a fluvial network that constitutes, at present, the offshore extension of modern rivers (the Seine, the Somme and the Solent) (Graindor, 1964; Larsonneur et al., 1975; Auffret et al., 1980; Gibbard, 1988; Hamblin et al., 1992; Bridgland, 2002; Antoine et al., 2003; Lericolais et al., 2003; Mellett et al., 2013; Tessier et al., 2013). These rivers acted as tributaries that merged during glacial low-stands into a larger river positioned off the present coast of Cotentin (Larsonneur et al., 1975; Benabdellouahed, 2013).

The coasts of Cotentin are characterized by sea-cliffs with elevations of ~ 100 m at Nez de Jobourg and less than ~ 4 m near Dielette (Fig. 1C). The cliffs alternate with sedimentary embayments underlined by pebble or shingle beaches and/or beach-ridges lying on sand (e.g. Ecalgrain embayment). At many sites, Quaternary continental deposits such as Holocene dunes or Pleistocene loess and periglacial deposits, known as heads, are overlying the terraces (i.e. Biville and Hatainville area, West Cotentin, North of Barneville-Carteret) (Lautridou et al., 1999).

The raised beaches and marine terraces from Cotentin have been extensively studied over 120 years (e.g., Bigot, 1897, 1898, 1930, 1931; Elhaï, 1960; Graindor, 1964; Pareyn, 1980; Scuvée and Alduc, 1981; Lautridou, 1983, 1985, 1989; Lautridou et al., 1999; Coutard, 2003; Coutard et al., 2005, 2006; Cliquet et al., 2009; Cliquet, 2015; Nexer, 2015). To the NE of the Peninsula (Fig. 1C), Coutard et al., (2006) described four terraces culminating at ~40 m; T1 has its shoreline angle (i.e. the intersection between the rocky platform and the fossil sea cliff of a marine terrace) at 6 ± 1 m NGF (the Principal Datum for France, Nivellement général de la France, see definition NGF section 3), T2's shoreline angle was measured at 17 ± 2 m NGF. The shoreline of T3 is present at 26 ± 2 m, and that of T4 at 31 ± 2 m, locally at 38 ± 1 m (Coutard et al., 2005, 2006). Based on five luminescence (OSL) datings on T1 coastal deposits sampled at the inner edge of the T1 terrace, Coutard et al. (2006) proposed to allocate T1 to T4 to the last four interglacials (MIS 5e, 7, 9, and 11). A submerged terrace, observed on bathymetrical charts at –20 m NGF at La

Mondrée site (LM on Fig. 1C) was interpreted as the geomorphic record of a sea-level stand during Marine Isotopic Stage (MIS) 5c or 5a (Coutard et al. 2006). Later studies focused on archaeology and environmental settings (e.g. Cliquet & Lautridou, 2009) using luminescence dating of the Middle Palaeolithic settlements at Gélétan, Anse du Brick, Port-Racine, Ecalgrain bay, and Le Rozel sites (Cliquet et al., 2003, 2009; Cliquet, 2015). MIS 7 deposits were described on T2 at Rocher Gélétan and on T1 on the North Ecalgrain Bay. The dating performed at Rocher Géletan was carried out on reworked burnt flint (*silex chauffé en position secondaire*, Cliquet et al., 2003) and impedes a confident correlation with MIS 7. At the Ecalgrain site, MIS 7 deposits have been described below those related to MIS 5e (Lautridou, 1983). A more recent study, including dating, proposed a reworking by periglacial processes of the MIS 7 coastal deposits on the MIS 5e platform (Cliquet et al., 2009).

Less attention has been paid to the coastal sequences of S Cotentin (Fig. 1B). To the SW, at sites Hacqueville and Hauteville-Annoville (sites 9 and 10 on Fig. 1B), the MIS 5e benchmark defines a strandline conforming to the modern one (Lautridou 1983, 1985, 1989; Lautridou et al., 1999). To the SE of the Seuil du Cotentin, a sequence of marine terraces is described at Grandcamp Maisy (site 19 on Fig. 1B; Lautridou, 1989; Coutard et al., 1979; Coutard and Lautridou, 1975), Asnelle Meuvaine (site 20 Fig. 1B; Bates et al., 2003; Pellerin et al., 1987) and Graye (site 21 Fig. 1B; Pellerin and Dupeuble, 1979).

Concerning the upper part of the sequence, marine deposits on the La Pernelle platform (NE Cotentin) were described at 90-110 m (Pareyn, 1980) but the outcrops were not further observed (Baize, 1998). The sediments described (Pareyn, 1980) are undated, azoic, supposedly marine deposits present at La Pernelle but also on the rasa south of Cherbourg (Hameau du Cloquant, La Glacerie, on La Boissais fossil island, see below) (Vérague, 1983). For the latter site, Vérague (1983) did a granulometric and chemical comparison with deposits from another outcrop in the area, and proposed a pre-Pliocene age for those deposits. Vérague (1983) noted that: i) their morphometric parameters are different from those of Cenomanian and Quaternary deposits, and, ii) their high kaolinite-content and depletion in silica suggests weathering under subtropical climates. In NE Cotentin, Coutard et al. (2006) described the lower part of the coastal sequence as overlooked by several high "continental plateaux" ranging from 90 to 150 m (Coutard et al., 2006). Bessin et al. (2015) also interpreted the upper surfaces of N Cotentin as continental in origin. In S Cotentin, Lautridou (1989) described Pliocene and Miocene coastal deposits ("Walton Crag") within the same area, to the NE of Hauteville-Annoville (site 10 Fig. 1B). Lautridou (1989) highlighted the relationship between the deposits and planation surfaces (that he named plateaux). Describing two planation surfaces (called rasas in this study) with Miocene and Pliocene deposits, he concluded that the platforms were not separated by faults which could be explained by their marine origin. Finally, 120 km southward of N Cotentin, in the Mayenne area (site Champéon and Saint-Denis–de-Gastines in Table 3 supplementary data), some outcrops are interpreted as Pliocene coastal deposits (which reworked older Cenomanian to Eocene deposits) overlying marine planation surfaces (i.e. rasas) (Gautier, 1967; Fleury et al., 1989). We emphasize that the rasas possibly reshaped antecedent continental planation surfaces, as some of them are overlain by scattered marine sedimentary remnants (see Bessin et al., 2015 for a review).

3 Background and methods

3.1 Late Cenozoic coastal staircase sequences and sea level

Late Cenozoic staircase sequences of coastal indicators develop concomitantly with sea-level changes on uplifting coastlines (Lajoie, 1986; Murray-Wallace and Woodroffe, 2014). The elevation of the shoreline angle (i.e. intersection between the rocky platform and the fossil sea cliff) of a marine terrace or a rasa (see below for definitions) provides a good approximation to the location and elevation of a former shoreline and, hence, a marker for relative sea level (Lajoie, 1986). The sequence corresponds to the geomorphic record of the Late Cenozoic high-stands (interglacial and interstadial) superimposed on an uplifting coast (Lajoie, 1986). At a global scale the formation of coastal sequences was likely operative since minima in the middle Miocene and locally (regionally) since the Eocene. The staircase shaping of coasts increased during the Pliocene and Pleistocene as a consequence of the intensification of eustatic sea-level oscillations (Pedoja et al., 2014), as inferred from the isotopic record (Lisiecki and Raymo, 2005).

3.2 Description of landforms

As rocky shore platforms, their modern counterpart, *marine terraces* are flat coastal surfaces bounded by steeper slopes, the inner slopes corresponding to a fossil sea cliff (Bradley, 1957; Bradley and Griggs, 1976; Lajoie, 1986). Marine terraces form as a result of coastal erosion ("wave-cut" terraces, i.e. a fossil rocky shore platform as in Bradley, 1957) combined with accumulation of shallow marine deposits (Murray Wallace and Woodroffe, 2014). Depending on the thickness of the coastal deposits on the fossil shore platform (more or less than 1-2 m) there is a distinction between a marine terrace and a wave-built terrace (Jara-Muñoz & Melnick, 2015). "Raised beaches" is old terminology (Dunlop, 1893) that corresponds to the coastal deposits associated with a marine terrace found emerged within the sea cliff and generally overlain by continental deposits. The *shoreline angle* of a terrace (or a rasa – see below) corresponds to the intersection between the fossil coastal platform and the fossil sea cliff. Its elevation is used in any quantification of tectonics or eustatic sea level (Lajoie, 1986).

Rasas are wide, elevated coastal planation surfaces corresponding to sequences of terraces wherein the shoreline angles are not observed. (see Fig. 2 in Pedoja et al. 2014). The word “rasa”, first used to describe such rocky surfaces on the northern coasts of Spain (Cueto and Rui Diaz, 1930; Hernandez-Pacheco 1950 both in Guilcher, 1974), was extended to landforms present in Morocco (e.g. Oliva, 1977), Tunisia (Paskoff and Sanlaville, 1983), Algeria (Authemayou et al., 2017), Lebanon (Sanlaville, 1974), Chile (e.g. Regard et al., 2010; Melnick, 2016), Peru and Ecuador (where rasa are locally named Tablazo e.g. Sheppard, 1927; 1930; Pedoja et al. 2006a, b), Costa Rica (Battistini and Bergoeing, 1982), eastern Canada (Allard and Tramblay, 1981) and Scotland (Dawson et al., 2013). Rasas are: 1) of polygenic origin - marine erosion occurred during various stands in sea level suggesting that re-occupation processes occurred on the rocky platform (Pedoja et al. 2006a,b; 2011; 2014; Regard et al. 2010; Dawson et al., 2013; Melnick, 2016; Authemayou et al., 2017); and 2) old features, as evidenced through direct dating; i.e. >0.5 Ma (e.g., Alvarez-Maron et al., 2008; Quezada et al., 2007) and most generally associated to areas experiencing low uplift (< 0.2 mm/yr; Pedoja et al. 2011, 2014; Melnick, 2016; ; Authemayou et al., 2017). In short, on slowly uplifting coasts, the formation of rasas was promoted before and during early Pleistocene times, during periods of faster oscillations and lower amplitudes in sea-level fluctuations than since the Middle Pleistocene.

Fig. 2 sketches a 3D idealized view of a coastal sequence similar to that of Cotentin which extends above sea level (rasa 1 to 4, Terrace T1 to 4), at sea level (T0 the modern shore platform) and below sea level (T -1). The terraces and rasas are defined as sub-planar, shallowly seaward–dipping surfaces between sea cliffs. T3 is a compound terrace; it locally includes a low fossil sea cliff (< 2 m) separating two terraces (T3' and T3" on Fig. 2). Marine cliffs are ~ 2 – 50 m high, and show two fossil islands (Fig. 2A). Depending on the paleogeography, uplift rates and the conservation of the landforms, the number of successive terraces observed in the landscape at a given point can vary drastically. The maximum number of emerged successive shorelines is 9 (not represented) including T3" and T3' (as on Transect IV, Fig. 2C) but on transect III and V this number is reduced to 2 and 3, respectively.

3.3 Mapping

High-resolution topography (LiDAR) and surface classification models were used to isolate remnants of marine terraces and rasas (Bowless and Cowgill, 2012). We used swath profiles and semi-automated mapping of the surfaces associated with the marine terraces and rasas using 5 -m-resolution topography (DEM Litto 3D, details in Nexer, 2015) combined with morphometric analysis. We developed a Surface Classification Model (SCM) to recognize terraced levels, as in Bowless and Cowgill (2012). Inputs into the model are the topographic slope and roughness, calculated herein as in Burrough and McDonnell (1998) and Frankel and Dolan (2007), using a

15x15 m roving-window (Fig. 3 A - D). The surface roughness is regarded as the standard deviation of slope of cells within the roving-window. Both topographic parameters were clipped from histograms (Fig. 3 E and F), using 90% of the distributions (15º slope and 4 roughness). The values above these thresholds, represented by gullies, valley slopes, and cliffs, are then removed to isolate the flat and smoothed surfaces characteristic of rasas and marine terraces (Fig. 3 B - D). Both truncated distributions were combined and normalized using a linear equation (Eq. 1) to create the SCM.

$$SCM = (SLP / SLP\_range)*0.5 + (RGH / RGH\_range)*0.5 \quad \text{(Eq. 1)}$$

where SLP and RGH are the surface slope and roughness, and SLP_range and RGH_range are the thresholds used to clip the topographic parameters. Then, the SCM was intersected with the topography to obtain elevation distributions studied using histograms and along profile projections. Marine terraces and rasas were isolated through elevation bands in histograms (Fig. 3, 4B-C), where the limits of these bands in histograms represent their inner and outer edges (Bowless and Cowgill, 2012).

Swath profiles were extracted perpendicular to terrace edges using TerraceM® (Jara-Muñoz et al., 2016); the maximum distribution of elevations on swaths was used to estimate the inner-edge (shoreline angle) elevations and for displaying the elevation patterns of rasa levels identified by the SCM.

3.4 Measurements of elevations

We focused our field efforts on North Cotentin. There, as elsewhere, the elevations of coastal landforms should be measured with reference to their modern counterparts, instead of in relation to a hydrological sea level which corresponds to the Principal Datum, characteristic of each country (Jardine, 1981; van de Plassche, 1986). The hydrographic sea level in France (NFG, IGN-1969, Nivellement Général de la France made by Institut Géographique National in 1969) is not sufficiently accurate for the Cotentin Peninsula (see Coutard, 2003; Nexer, 2015). Consequently, for the measurements of elevation from barometrical altimeters, we generally tied the elevation measurements to the modern shoreline angle (break of slope between the modern platform and the sea cliff) that correspond to the *morphological* sea level and performed repeated measurements. We also measured the elevations of shoreline angles with differential GPS (Global Positioning System), also repeatedly when possible. We used a Trimble Geoexplorer 2008 (horizontal and vertical precision of 1 m) and we made our measurements according to the French P.D. that was also tied to the morphological sea level (Table 1). The Cotentin Peninsula area is macro-tidal and we assume that the tide range remained steady through the period of time covered by our study even if changes in coastal paleogeography such as those evidenced herein may have induced changes in tidal amplitudes. We assigned an error to each measurement depending on the preservation of fossil shorelines. These errors increase with the elevation and degradation of the coastal indicators, from 1-2 m for the low-standing terraces to up to 10 m for the uppermost rasa.

3.5 Sea-level curves used and uplift rates

Several Quaternary sea-level curves have been derived from the isotopic and/or geomorphic records (Waelbroeck et al., 2002; Lisiecki and Raymo, 2005; Siddall et al., 2006; Zachos et al., 2008; Bintanja and Van de Waal, 2008; Rohling et al., 2009; Murray-Wallace and Woodroffe, 2014). For each MIS, the sea-level curves vary by several thousand years (ka) in age and by several metres in height, that collectively yield some inaccuracies when used (Caputo, 2007). Nevertheless, there is relative consensus on the succession and ages of the most recent high-stands.

The most commonly investigated high-stand in the geomorphological record is the last interglacial period allocated to MIS 5 (e.g., Stirling et al., 1998; Murray-Wallace and Woodroffe, 2014), and which includes three relative high-stands, MIS 5a (85 ± 5 ka), MIS 5c (105 ± 5 ka) and MIS 5e (128 ka to 116 ka). MIS 7 ranges from 190 to 245 ka (Thompson and Goldstein, 2005), and includes sub-stages 7a, 7c and 7e (Dutton et al., 2009). Two sea-level high-stands occurred within MIS 9, sub-stages 9a and 9c extending from 306 ± 3 ka to 334 ± 4 ka respectively (~ 324.5 ± 18.5 ka; Stirling et al., 2001). MIS 11 lasted from 420 ka to 360 ka (Murray Wallace and Woodroffe, 2014). Earlier interglacials are MIS 13 (480-530 ka), MIS 15 (560-620 ka) and MIS 17 (650-720 ka; Thompson et al., 2003; Andersen et al., 2008; Murray-Wallace and Woodroffe, 2014). Fewer agreements exist in regards of the position of the sea level during Pleistocene high-stands with respect to present (i.e eustatic sea-level) and the estimates vary drastically. We compared the values from the last global compilation of geomorphic Quaternary sea-level indicators (Murray-Wallace and Woodroffe, 2014) with five eustatic sea-level curves (Table 1). The curves selected (Waelbroeck et al., 2002; Bintanja and Van der Wal, 2008; Grant et al., 2014; Shakun et al., 2015; Spratt and Lisiecki, 2016) encompass different reconstruction methods, cover the time-range of interest (since MIS 11, 420 ka), and have their uncertainties quantified. Murray-Wallace and Woodroffe (2014) analysing considerable amount of literature, proposed that MIS 5e, MIS 7, MIS 9, and MIS 11 sea level high-stands were, respectively, 6 ± 4 m higher, -8 ± 12 m lower, 3 ± 2 m higher, and 9.5 ± 3.5 m higher than the modern sea level (Table 1). Waelbroeck et al. (2002) built a composite relative sea-level curve over the last four climatic cycles from long benthic isotopic records retrieved at one North Atlantic and one Equatorial Pacific site. Bintanja and Van der Wal (2008) used both ice-sheet and ocean-temperature models to extract 3 Ma mutually consistent records of surface air temperature, ice volume and sea level from marine benthic oxygen isotopes. Grant et al. (2014) proposed a chronology derived from a U/Th-dated speleothem $\delta^{18}0$ record, for a continuous, high-resolution record of the Red Sea relative sea level over five complete glacial cycles (~ 500 ka). Shakun et al. (2015) compiled 49 paired sea surface temperature-planktonic $\delta^{18}0$ records and extracted the mean $\delta^{18}0$ of surface ocean seawater and eustatic sea level over the past 800 kyr. Finally, Spratt and Lisiecki (2016) performed principal component analysis on seven records from 0 to 430 ka and five records from 0 to 798 ka (Spratt and Lisiecki, 2016).

Based on previous dating and our elevation measurements for the Pleistocene shoreline angle, we derived uplift rates for North Cotentin. Eustasy-corrected uplift rates are given by dividing the difference between the elevation of the shoreline angle of dated marine terrace and the eustatic sea level at the time of its formation by the age of the terrace (Lajoie, 1986). We also calculated the *apparent* uplift rates that neglect any *a priori* eustatic correction (as in Pedoja et al., 2011; 2014; Yildirim et al., 2013; Authemayou et al., 2017) (Table 1).

3.6 Modeling the lower part of the sequence

To propose ages for the undated low-standing marine terraces, T2 to T4, on the Cape de la Hague (NW Cotentin), we used a synchronous correlation method as in Roberts et al. (2013). We attempted to estimate uplift rates by searching for the best match between the measured elevations of the successive shoreline angles with those obtained by extrapolating uplift rates to the entire sequence of landforms. This method initially assumes constant uplift rate, but with the option to test varying uplift rates over time (Roberts et al., 2013). The Terrace Calculator is initially driven by age controls. We extrapolated a fixed uplift rate of 0.01 mm/yr based on the Last Interglacial Maximum (MIS 5e) dated terrace (122 ± 6 ka), present at elevations of ~ 5 ± 1 m. The output is the expected inner-edge elevations of the terraces allocated to the high-stands from a chosen sea-level curve. These modeled shoreline angle elevations are then matched against the measured one. Crucially, this method takes into account re-occupation processes, i.e. old terraces can be erased by subsequent high-stands, especially in a low uplifting area (e.g., Westaway, 1993; Roberts et al., 2013). Herein, the Terrace Calculator relies on the sea-level curves from Siddall et al., (2003) for 0-410 ka and Rohling et al. (2014) from 410-980 ka in the form of sea-level relative to present-day and high-stand ages. To compare with estimates from other sea-level curves, we used data from: Murray-Wallace and Woodroffe (2014) from 0-400 ka, Grant et al. (2014) from 0-480 ka, Waelbroeck et al. (2002) from 0-478 ka and Rohling et al. (2014) from 0 to 980 ka. Sea-level data from this latter curve were also used to supplement the data within other models from their upper age limits to 980 ka (see section 3.1).

3.7 Database on Western European strandlines

We expanded on Pedoja et al. (2011, 2014) databases on Cenozoic sequences of strandlines that focused on MIS 5e and MIS 11 high-stands (supplementary data Table 1). Here, we also provide information about: 1) sites where some MIS 7 landforms are present but landforms allocated to MIS 5e are lacking (supplementary data Table 2): and 2) Neogene fossil shorelines (supplementary data Table 3).

4 Coastal uplift of the Cotentin Peninsula

4.1 Distribution of the coastal sequences

Our analysis reveals that the coastal sequences extend all over the Cotentin Peninsula on a >200-km-long coastal stretch (Fig. 4-6). Depending on the occurrence of the lower part of the sequence (i.e. marine terraces), we subdivided the peninsula into three areas (Fig. 4A). North Cotentin is circumscribed by the English Channel and the low-rising margin of the Seuil du Cotentin basin. South Cotentin is located south of the Seuil du Cotentin basin. In between these two areas, in the Seuil du Cotentin basin, no marine terraces are obvious in the landscape (Fig. 4A) but: **1)** interglacial coastal deposits have been described using data from a borehole (see section 4.4.3.); **2)** some rocky hills exhibit flat tops that we interpreted as shaped by coastal erosion (emergence of rocky islets and platforms); and **3)** surface classification model shows that the Seuil du Cotentin basin is a flat area, with a mean elevation similar to that of the low lying terraces present in North and South Cotentin (Fig. 3, 4A-C).

4.1.1 The lower marine terraces: T1 to T4

Along the shores of N Cotentin, the lower part of the sequence is laterally continuous over ~110 km (Fig. 4D), from Saint-Vaast-la-Hougue in the Val de Saire area (east), to Carteret (west). Such successive low-standing marine terraces are lacking where elevated sea-cliffs are present, i.e. between the Nez de Jobourg and the north of Anse de Vauville (Fig. 1C, 4D). The terraces and their deposits are frequently capped by thick Pleistocene heads and loess (as in the Baie d'Ecalgrain, Fig. 4A) or are heavily reworked by human activities (urban area of Cherbourg, Fig. 4A, 4E). The width of the low part of the sequence (T1 to T4 marine terraces) ranges from a few tens of metres (for instance at Port Racine) to a maximum of 6 km (Val de Saire). The lower part of the sequence is the widest within the embayment (1 km at Urville bay) and on Cape de la Hague (1.5 km). At the Cap de la Hague, from La Roche (see Fig. 6A) to Port Racine, only the three lowest marine terraces are well expressed in the landscape. T4 is locally present to the west (north of Auderville) as a residual landform (paleo-peninsula or paleo-island?). Between Goury and Rocher Gélétan (Fig. 5B), the lower strandlines have been eroded (i.e. formation of a low-standing rasa). In the area, the 50 -to- 500 -m-wide T1 terrace has its distal edge at 5 ± 1 m NGF (2 ± 1 m above the modern shoreline angle; Table 1). Its shoreline angle culminates at 7 ± 1 m NGF (5 ± 1 m above the modern shoreline angle). T2, as T1, is 50 to 500 m wide. Its distal edge is present at an elevation of 10 ± 2 m NGF (7 ± 2 m above the modern shoreline angle) whereas its shoreline angle is present at 15 ± 2 m NGF (12 ± 2 m above the modern shoreline angle). On the Cap de la Hague (Fig. 5A-B), T1 and T2 strandlines conform to the modern shoreline; fossil beach deposits and fossil sea stacks are associated to this terrace at Rocher Geletan and Hâvre de Bombec sites (Fig. 5B), for example. On the Cap de la Hague, we observed deposits associated to T1 marine terrace at 23 sites. These deposits are either 0.5 to 1.5 m -thick layers of beach deposits comprised of a sandy matrix embedding sometimes sorted centimetric to decimetric pebbles, suggesting only minor periglacial reworking, and thinner deposits (0.5 m) of clay and silt with only a few metres of lateral extent. These coastal deposits were reworked or capped by posterior periglacial processes (solifluction) (Fig. 6B). T3 is 100 to 900 m wide and its distal edge is found at 17 ± 2 m above the modern shoreline angle (20 ± 2 m NGF). The shoreline angle of T3 culminates at 22 ± 3 m above the modern shoreline angle (25 ± 3 m NGF). Its strandline does not conform to the modern one as it forms a fossil cape at the Rocher Gélétan site (Fig. 5B). Finally, we infer the presence of T4 as a relict island or point on the western side of the Cape de la Hague. The surface associated to T4 is present at ~33 ± 3 m.

4.1.2 The upper rasas, R1 to R4

All over the Cotentin Peninsula, we recognized four flat surfaces above the low-standing marine terraces (Fig. 3 - 6). These surfaces are displayed over kilometres and exhibit staircase morphology as they are separated by cliffs.

In N Cotentin, the sequence culminates at 185 ± 10 m (see rasa 4 on Fig. 4D). The toe of the cliffs separating the staircase surfaces (i.e. rasas 1 to 3 of this study) are respectively found at 167 ± 5 m 138 ± 5 m and 86 ± 5 m (Fig. 4E). We discard the hypothesis that such surfaces are the results of long-term periglacial weathering of pre-existing continental surfaces. In our opinion, such weathering is unlikely to generate regular staircase surfaces with similar elevations for each step (i.e. each rasa) all over the peninsula. On La Hague Point (not to be confused with the Cap de la Hague, the northern tip of La Hague Point), some of these cliffs were interpreted as fault scarps associated with a NW - SE fault (Font et al., 2002; Lagarde et al., 2003). However, morphologic and morphometric evidence suggests that these landforms are fossil sea-cliffs not fault scarps. i) These cliffs, present on the interfluves, are continuous in the landscape and on the DEM and not only observed on La Hague Point (Fig. 4). Each individual cliff exhibits a circular or oblong pattern. From map view, the outline shape of successive cliffs most generally conforms to the lowest one and defines a concentric circular, or oblong, staircase coastal landscape as observed for example on La Hague Point, to the south of Cherbourg, or to the east of Barneville-Carteret (Fig. 4A). Such geometries (Fig. 4A) are difficult to relate to the geometry of faults. ii) The inner-edge elevations of the planation surfaces suggest that there are no elevation offsets at both sides of the Hague Point (Fig. 7A, B) indicating that no tectonic movements took place along a purported fault running along the elongated top of the Hague Point. In addition, we compared cliff heights and their corresponding inner-edge elevations of each rasa level obtaining positive correlations (Fig. 7C). Following the criteria proposed by Jara-Muñoz et al., (2017), positive correlation suggests that these scarps were formed by the effect of coastal erosion and uplift. In contrast, fault scarps usually characterized by negative or no correlation. iii) Tectonic displacement due to this purported fault has been evoked to explain the difference of elevations of the MIS 7 deposits at Ecalgrain and the MIS 5e deposits on La Hague Point. Recent dating of the Ecalgrain deposits suggest a reworking of MIS 7 deposits on the MIS 5e platform (i.e. re-occupation) (Cliquet et al., 2009; Cliquet, 2015) which does not imply any activity of the purported fault.

In coastal areas, staircase flat surfaces with a circular or oblong pattern of the successive cliffs are interpreted as the uplift and emergence of an island that further coalesced with the nearby mainland (e.g., Szabo and Wedder, 1971; Lajoie et al. 1991; Pedoja et al., 2006 a,b; 2014; Authemayou et al., 2017). Hence, we interpret the staircase planation surfaces of the Cotentin peninsula as rasas with their associated shoreline angles.

In S Cotentin (Fig. 4F), the shoreline angles of the rasas R1 to R3 were found at similar elevations within the error range of measurements to that of N Cotentin: 83 ±

5 m, 136 ± 5, and 167 ± 5 m. Rasa 1 is best observed south of Avranches where it constitutes wide surfaces (> 3km). Rasa 2 is the most extensive surface in the area (width reaching 10 km) and Rasa 3 is morphologically better developed than in N Cotentin. Rasa 4 caps the highest parts of the S Cotentin Peninsula with its distal edge at 174 ± 5 m and its inner edge at 200 ± 5 m. The strandlines demonstrate a convex segment of the coast (i.e. paleo-capes) locally interrupted by narrow embayments, such as that observed east of Avranches.

4.2 Paleogeographical evolution

The distribution of the fossil strandlines in Cotentin provides strong evidence for the emergence and coalescence of various rocky islands and islets, i.e. a rocky archipelago, to form a bigger island that latter connected to the mainland through the closure of the "Seuil du Cotentin" seaway. Such evolution began with the uplift of rocky reefs and platforms to form the first islands of the archipelago. The size of such islands typically ranges from few tens of metres to few kilometres with various shapes; La Hague fossil island is oblong whereas La Boissais fossil island is more circular. Such rocky platforms and low-lying islands compare with the modern Chausey archipelago (Fig. 1B). Subsequently, the uplift concerns larger, flat rocky islands bordered by shore platforms comparable to Alderney Island (Fig. 1B). The islands further expand in size by the formation of successive rasas, and latterly marine terraces leading to larger and higher islands (as in Fig. 2) comparable to

Guernsey or Jersey where elevated marine terraces are also known (see Fig. 1B, Renouf and James, 2011). Neighbouring rocky platforms result in the coalescence of various elevated islands: six on N Cotentin and two overlooking the SW side of the Seuil du Cotentin Basin (Fig. 4D). Through the closure of the Seuil du Cotentin seaway, the N Cotentin main island (Rasa 1) was connected with the landmass, to form the Cotentin Peninsula. This evolution is somehow schematic owing to the interplay of tectonics, continental and marine erosion during earlier times, including terrace re-occupation processes or, in theory, the emergence of terraces formed during sea-level low-stands.

In summary, in N Cotentin the strandlines associated with the rasas define fossil rocky islands and islets, while to the south of the Peninsula they define the landmasses at the time of the emergence of the northern islands. We did not find Cenozoic marine deposits associated with the rasas but they have been described both to the north and south of the Peninsula (section 2.2).

4.3 Upper Pleistocene (MIS 5e) uplift rates revisited

We focused on dated terraces for which the elevations of the shoreline angles are measured directly above their modern counterparts and calculated uplift rates for the MIS 5e benchmark in N Cotentin. At various sites, its elevation above its modern counterpart (~ 5 ± 1 m) implies an apparent uplift rate of 0.04 ± 0.01 mm/yr (Table 1). The mean eustasy-corrected uplift rates have large margins of error (Table 1). Depending of the sea-level data used, their mean values can be either: i) slightly negative: -0.01 ± 0.04 mm/yr (data from Murray-Wallace and Woodroffe (2014)), ii) neutral: 0.00 ± 0.11 mm/yr (data from Waelbroeck et al. (2002) or 0.00 ± 0.13 mm/yr (data from Spratt and Lisiecky (2016)) or iii) positive: 0.04 ± 0.08 mm/yr, 0.13 ± 0.12 mm/yr and 0.01 ± 0.12 mm/yr (data from Bintanja and Van Der Wal (2008), Shakun et al. (2015) and Rohling et al. (2014) respectively). As previously noted for the sequence of NE Cotentin, subsidence is unlikely since the coastal staircase morphology is clearly associated with uplift (Coutard et al., 2006). For T1 and T2, an error of ± 12 m for the predicted elevations for each high-stand is directly taken from Siddall et al. (2003). T3 and T4 have a higher error of 35 m as per the discussion in Rohling et al. (2014). As some of these errors are larger than the elevations of the terraces used, we applied statistical testing to interpret the relationship between a set of predicted elevations versus measured elevations (see below).

Whichever correction is applied, Upper Pleistocene coastal uplift rates are low to very low (< 0.2 or <0.1 mm/yr, respectively, as in Pedoja et al. (2011)) as observed elsewhere along the Western European coasts (section 5.3) or along other passive margins (Pedoja et al., 2014).

4.4 Possible timings for the emergence of the Peninsula

To obtain a chronological framework for the undated landforms, we postulated steady uplift rates (Lajoie, 1986), although this is unlikely at the timescales considered. We extrapolated three possible rates derived from: (i) the elevation of the dated MIS 5e terrace; (ii) the elevations of T2 to T4 allocated to MIS 7, 9 and MIS 11 (short lasting hypothesis, as in Coutard et al., 2006) (Fig. 8A) and; (iii) modelling of the lower sequence (long lasting hypothesis, Fig. 8B, 9). These are further explored below.

4.4.1 Short-lasting hypothesis

In N Cotentin, the "standard method" (Table 2) which sequentially correlates each subsequently higher terrace to the next older high-stand, consists of the allocation of T2, T3 and T4 to MIS 7, MIS 9 and MIS 11, respectively (as in Coutard et al., 2006). It results in homogeneous apparent uplift rates (~ 0.06 ± 0.03 mm/yr; Table 2). When corrected for eustasy, variations in the uplift rates are clear and show an increase of uplift during the penultimate interglacial whatever the correction applied (Table 2, Fig. 8A). Consequently, we extrapolated a mean MIS 5e apparent uplift rate of 0.04 ± 0.01 mm/yr, and a mean "high" Middle Pleistocene eustasy-corrected of 0.09 ± 0.03 mm/yr (Table 3).

On N Cotentin, rasa 4 caps the paleo-islands of La Hague and La Boissais at elevations of 185 ± 10 m (Fig. 8A). Both islands would have emerged at 5 ± 1.5 Ma (apparent) or 2.9 ± 0.9 Ma (eustasy-corrected) (see Table 3 for the possible age of formation of the other rasas). In summary, the short-lasting hypothesis suggests a Pliocene onset of the sequences preserved on the peninsula.

4.4.2 Long-lasting hypothesis

Synchronous correlation modelling (as in Roberts et al., 2013) suggests that a constant uplift rate of 0.01 mm/yr (Table 4) would be responsible for the formation and preservation of the four low terraces (T1-T4) on N Cotentin. The shoreline angle of the last interglacial maximum T1 marine terrace is found at ~ 5 ± 1 m above its modern counterpart and has a predicted elevation of 6 m. Modelling suggests that T2 (at 12 m) would be correlated with the 340 ka high-stand (MIS 9c, predicted to be at 8 m). T3 (at 22 m) would be allocated to either the MIS 13 (525 ka) or MIS 15 (620 ka) high-stand predicted to be both at 26 m (Table 4, Fig. 8B and 9). Finally, T4 (at 33 m) would be assigned to the 980 ka high-stand predicted to be at 35 m. The modelling suggests reoccupation processes for the high-stands between MIS 5e and MIS 9c, as well as for those between MIS 9c and MIS 15 (numbers in grey scale, Table 4). Such processes, symptomatic of low uplift, have also been observed at Menez

Dregan (W Brittany, Table 1 supplementary data) where both MIS 5e and MIS 11 coastal deposits are present on the same terrace. In our analysis, T2 was allocated to the MIS 11 high-stand using eustasy-correction from either Waelbroeck et al. (2002) (predicted to be at 10 m) or Murray-Wallace and Woodroffe et al. (2014) (predicted to be at 14 m). As sea-level data from these curves does not extend beyond 478 ka, the allocations of T3 and T4 did not alter when they were tested. We assessed the relationship between the predicted and measured elevations using a non-parametric method – Pearson's correlation coefficient with an output of r = 0.99, approaching the ideal value of 1 (Fig. 9A). This indicates a robust correlation between multiple strandline elevations and multiple sea-level high-stands, which would imply that uplift rates have not varied over the last 0.5 Ma.

We compared the RMS deviation of all uplift rates scenarios from 0 to 0.11 in intervals of 0.005 in order to assess the accuracy of the constant uplift rate we obtained from the dated shoreline (Fig. 9B). An uplift rate of 0.01 mm/yr constant over ~ 1 Ma provides the best fit uplift rate to model the coastal sequences of the Cotentin Peninsula (Fig. 9B). Extrapolating such a rate yields that Rasa 4 would have emerged at 18.5 ± 1 Ma, Rasa 3 at 16.5 ± 0.5 Ma, Rasa 2 at 13.8 ± 0.5 Ma and Rasa 1 at 8.6 ± 0.5 Ma (Table 3, Fig. 8C). Assigned rasa ages are in good agreement with Neogene-aged high-stands (Miller et al., 2005). R4, R3 and R2 would record the following highstands; ~ 17.5-18.5 Ma (early Miocene), 14.5 Ma (middle Miocene), 13.5 - 12 ka (late Miocene). Finally, R1 would be the morphological expression of the intensification of the sea-level oscillations during the late Miocene-Pliocene and early Pleistocene.

In short, the long-lasting hypothesis emphasizes an early Miocene onset of the coastal sequence preserved on the Cotentin Peninsula.

4.4.3 Age of the onset of the coastal sequences?

Both uplift hypothesis (i.e. short versus long-lasting) fit with previous descriptions of Miocene and Pliocene coastal deposits overlying the rasas (see section 2.1). The combination of hypotheses results in a very large age range. Rasa 4 would have emerged between 1.5 and 19.5 Ma considering all the errors within the extrapolation (Table 3).

The timing of the closure of the seaway that once formed the Seuil du Cotentin area provides crucial data to assess the age of the coastal sequences located in its vicinity. Based on boreholes and sparse outcrops, the thickness of the marine to fluvial sediments deposited in the Seuil du Cotentin basin is estimated to be > 150 m. The sediments consist of clastic deposits with conglomerates and peat at the top of the formation. The depositional environments of the succession change from marine to fluvial and represent two transgression–regression cycles (Dugué, 2003). In many studies (Clet-Pellerin et al., 1997; Garcin et al, 1997; Dugué et al., 2007, 2009) this sequence is interpreted as being deposited during Late Pliocene to Early Pleistocene. The first transgression identified is referred to as the "Brunssumian–

Reuverian", which approximates to the whole Pliocene and the associated deposits are now found offshore in the English Channel (Dugué, 2003). The second transgression is proposed to be Lower Pleistocene (Tiglian, 2.4-1.8 Ma) associated with the Sable de Saint Vigor Formation. Clet-Pellerin et al. (1997) proposed an age of 1.45 - 1.2 Ma (MIS 34 - 36) in comparison with other European sites. However, the exact correlations between these local stages and the international chronological stages remain unknown. More recently, van Vliet-Lanoë et al. (2002) proposed for the Sable de Saint Vigor, through direct Sr dating, a Zanclean (Pliocene) age for the formation.

At this stage, more dating is needed to better constraint the timing of the onset of the coastal sequences preserved on the Cotentin Peninsula.

5 Late Cenozoic uplifting coastal sequences of Western Europe

Early descriptions of marine terraces and raised beaches arise from the English Channel shores mostly because low-standing coastal deposits and overlying continental cover both contain flints and extinct mammal bones (e.g Lyell, 1830; Moore, 1842; Chambers, 1848; Prestwich, 1862-1863; Breuil et al., 1942). Early syntheses on sequences of strandlines dealt with Western Europe and more specifically with sites in western France and southern England (e.g., Barrell, 1915;

Depéret, 1918-1922; Daly, 1925; Wythe-Cooke, 1930; Bull, 1941; Baden-Powell, 1954; Guilcher, 1969). This area is rather neglected in recent global synthesis on sea - level changes (e.g. Pedoja et al., 2014; Murray-Wallace and Woodroffe, 2014).

Out of 180 references (supplementary data Tables 1, 2, 3), we evidenced: 1) 169 sequences embedding the MIS 5e benchmark (99 sites in Pedoja et al. 2014), 2) two sequences including coastal landforms and deposits correlated to MIS 7 but no strandline correlated to the last interglacial maximum (MIS 5e), 3) 14 sequences including the MIS 11 shoreline; and 4) 21 sequences including some Neogene strandlines.

At any coastal site, current elevations of the Holocene and Pleistocene terraces depend on the combination of glacio-isostatic adjustment (GIA), tectonics and other local processes (Shennan and Horton, 2002; Milne et al., 2005). In France, Spain and Portugal, the lack of accurate Holocene sea-level index points precluded the establishment of Holocene sea-level curves but recent advances have been made from the analysis of submerged deposits in estuaries (e.g., Leorri et al., 2012). Lambeck, (1991; 1996) and Shennan and Horton, (2002) constrained Late Pleistocene and Holocene relative sea level changes in the British Isles and provided estimates of current land-level changes (negative of relative sea-level change). Maximum relative land uplift occurs in central and western Scotland, at ~ 1.6 mm yr^{-1}, and maximum subsidence is in southwest England, at ~1.6 mm yr^{-1}. As our aim is to evidence the Neogene - Quaternary tectonic uplift of western European coasts, we do not consider, in our interpretation, sequences located in areas where fast GIA dominates the signal, as evidenced by Lambeck (1987; 1991) and Shennan and Horton (2002; see dotted line Fig.10A). In area where the last GIA is inducing subsidence (i.e. Southern England), tectonic uplift is lowered. Of course such quantifications only concern the period following the last glacial (MIS 2). In the case of MIS 5e marine terraces, two joint corrections could be applied because one should ideally compare the shape of the Earth deprived of GIA, therefore compare a GIA-relaxed MIS 5e (i.e. without any GIA from the previous deglaciation stage MIS 6), with a present-day GIA-relaxed Earth. This lack of knowledge on Middle Pleistocene GIA prevents correcting MIS5e uplift rates. Consequently for the British Isles, we discarded 64 sites (underlined in grey on supplementary Table 1) where older, Middle Pleistocene highstands (MIS 7, 9, MIS 11) are absent and where MIS5e is not embedded within a longer lasting sequence.

At many sites along the coasts of Spain, Portugal and France, sequences are morphologically similar to that of Cotentin: low-standing, rather well-individualized fossil rocky strandlines, overlooked by older, wider rasas. In NW Portugal (Minho area), five marine terraces reach 65 ± 5 m in elevation and are overlooked by a rasa culminating at 100 m (e.g., Texier and Meireles, 1987). In France, within the Brest embayment (Feunteunaon site Table 1 Supplementary data), a sequence of six terraces and rasas reach 135 m in elevation (Guilcher, 1974; Hallégouët, 1976). Fossil landforms frequently consist in rocky shore platforms with associated deposits (e.g., rasa and marine terraces), sea caves with coastal deposits (e.g. Sutcliffe et al., 1987), or fossil depositional landforms such as the Plovan beach ridge (Guilcher and Hallégouët, 1981). Most sequences are strongly affected by continental erosion. Remnants of marine terraces and rasas, preserved on the interfluves, are often capped by continental deposits: heads and loess to the north (e.g., Regnauld et al., 2003), aeolian and alluvial deposits to the south (e.g., Teixeira, 1944). In Spain and Portugal, rasas are obvious in the landscape and frequently include coastal deposits. In France, rasas are more dissected and show fewer deposits that are often azoic. Rasas, whether sedimentary (e.g., Portugal, see Cunha et al., 2015a, 2015b) or erosive, are more intensely dissected by fluvial erosion than younger marine terraces (for instance in the Pays de Leon, Brittany, e.g., Hallégouët, 1976). Within estuaries, sequences are composite, made of both marine and fluvial terraces, as observed in Portugal (e.g., Ramos et al., 2012), Spain (Moreno and Mediato, 2009), France (e.g., Hallégouët, 1976) or England (Westaway et al., 2009).

Dating indicates that the lowest standing coastal landforms were formed during MIS 5e high-stand (Table 1 supplementary data) for which we compiled its elevation at 169 sites. Two studies propose a different morpho-stratrigraphy for some marine terraces deposits in Portugal and Spain. On the basis of ^{14}C and OSL dating, Benedetti et al. (2009) correlated some of the low-standing terraces in Estremadura

(Portugal) to MIS 3 and 4. Through ^{14}C dating, González-Acebrón et al., (2016) also correlated low-standing terraces to MIS 3 in southern SE Spain, next to Cadiz. We discard these results since they are not benchmarked on the same MIS 5e, MIS 11 or older sea level high-stands that we consider herein.

At two sites, strandlines older than MIS 5e are present whereas MIS 5e is lacking (Fig. 10B and Table 2 supplementary data). At Sangatte (N France), long-recognized coastal deposits and morphologies (e.g., Prestwich, 1851, 1865; Baudet, 1959), were dated by OSL and correlated to MIS 7 (Balescu et al., 1992), but the sedimentary coastal sequence could also include MIS 9 deposits (Sommé et al., 1989; 1999). At Easington (Eastern England), in an area affected by post glacial rebound (uplift) raised beach deposits associated to a fossil strandline were dated by OSL and amino-acid racemization and correlated to MIS 7 high-stand (Davies et al., 2009). Older dated geomorphic markers consist in MIS 11 strandlines, described at 14 sites (Table 1 supplementary data). Finally, rasas overlook individualized strandlines at 21 sites (Fig. 10C, Table 3 supplementary data). At a limited number of sites in SW Europe, marine deposits or marine surfaces associated with the rasas have been dated (Fig. 10C, Table 3 supplementary data). The dating is absolute (^{10}Be; Sr) as for the Rasa of Cerro da Boa Viagem (Portugal) or the 60 m-high rasa of Cantabria (Spain) or relative (biostratigraphy, geometry of discordance, etc.) (Table 3 supplementary data). A Miocene (Aquitano-Langhense) onset is proposed for the sequence of central and western Asturias (Spain) where the highest rasa has an elevation of 264 m and 180 m, respectively (Table 3 supplementary data). In Portugal, the onset of the sequences is proposed to be Pliocene (Table 3 supplementary data, sites Serra da boa Viagem, Lavos-Alqueidao, Maiorca - Vila Verde or Cabo Espichel for example). Comparison with similar sites around the world shows that Pliocene or Miocene ages for the initiation of some coastal sequences are still discussed, for example in Casablanca, Morocco (Raynal et al., 1999).

Within the studies compiled, elevation measurements are generally provided above the Principal Datum of the considered country (e.g., NGF for France, O.D. for England; see section 2.2). Yet, studies where elevations measurements are discussed are scarce (e.g., Arkell, 1943; Alonso and Pages, 2000; Coutard et al., 2006; Figueiredo et al., 2013).

At various sites, the mean elevation of the shoreline of the last interglacial maximum stands within estimates for the eustatic range of MIS 5e sea level with respect to present-day (Siddall et al., 2006; Kopp et al., 2009; Rohling et al., 2009). However, in Western Europe as elsewhere (Pedoja et al., 2014; Authemayou et al., 2017), MIS 5e marker is always embedded within a staircase coastal sequence, a morphology that cannot be explained in the absence of regional uplift.

Excluding areas affected by fast GIA, in our database, the elevation of MIS 5e benchmark ranges from -2 ± 1 m (site Le Havre, France, Breton et al., 1991) to 19.5 ± 1 m at Tarifa (Atlantic Southern Spain, Zazo et al., 1999) with a mean of 6.2 m ± 1.6 m (Table 3 supplementary data). Elevations of Middle Pleistocene MIS 11 landforms range from 8 ± 3 m to 33 ± 4 (mean 20 ± 2.5 m). Consequently, upper Pleistocene (MIS 5e) apparent uplift rates range from - 0.016 ± 0.008 mm/yr to 0.16 ± 0.01 mm/yr with a mean of 0.05 ± 0.01 mm/yr (Fig. 10A). Apparent Middle Pleistocene uplift rates range from 0.02 ± 0.01 to 0.08 ± 0.02 mm/yr (mean 0.05 ± 0.01 mm/yr) (Fig. 10B). The modern elevation of rasas indicates long-term tectonic uplift of Western Europe (Spain, Portugal, France, and possibly UK and Ireland) as such landforms cannot be explained by the sole effect of eustasy. Mean apparent long-term uplift rates are ~ 0.01 mm/yr, (Table 3 supplementary data, Fig. 10C) and are consistent with previous estimates of ~ 90 m of Pleistocene uplift from fluvial incision measurement in the coastal area (ca. 0.03 mm/yr; Bonnet et al., 2000; Brault et al., 2004).

Pleistocene and Neogene coastal uplift rates of Atlantic Europe are low to very low (~ 0.01 to 0.2 mm/yr, as in Pedoja et al., 2011) and rather uniform over the studied zone, though with local exceptions that we cannot address without further dating (e.g., MIS 7 at Sangatte, see Table 1 supplementary data). At first glance, the convergence between Eurasia and Africa induces more intense deformation to the south in southern Spain and Portugal (e.g. see Ingrina or Conil-Trafalgar data, Table

1 supplementary data). But, before any detailed interpretation, these data need to be refined especially for rasa sites where deposits are present.

Our findings are in line with earlier studies that suggest that a Neogene tectonic event affected most continental margins of Atlantic Europe, and reached far into the European craton (e.g., Japsen and Chalmers, 2000). Similar vertical movements are reported for other continental margins (e.g., Japsen et al., 2006; Bonow et al., 2009), and are not unique to the Late Cenozoic (Peulvast et al., 2008; Bertotti and Gouiza, 2012). These facts taken together call for a common underlying process. These anomalous vertical motions ought to have a large-scale tectonic origin, regardless of the subjacent proposed mechanism, which remains a matter of debate. Possible mechanisms are igneous underplating (Brodie and White, 1994), asthenospheric upwelling, isostatic readjustments due to glacial erosion and regional compression of the lithosphere (e.g. Japsen and Chalmers, 2000; Yamato et al., 2013). We favour the latter for it fits with the large-scale distribution of the coastal uplift evidenced from southern Spain to Northern Ireland (Fig. 1A, 10). In an attempt to reframe the Atlantic coastal uplift of Europe in its entirety, we emphasize that, alike mountain belts worldwide, uplifting coasts of western Europe are symptomatic of the generalized lithospheric compression that increased during the Cenozoic (Yamato et al., 2013). Collisions at far-field plate margins overall increase compression in lithospheric plates; tectonic inversion, and uplifting continental margins reveal this augmenting stress regime worldwide (Pedoja et al., 2011; Japsen et al., 2012; Yamato et al., 2013). Similar regional illustrations are found in Greenland (e.g., Døssing et al., 2016), southern Africa (Green et al., 2016), or Brazil (Japsen et al., 2012). Ultimately, this compression is induced by mantle convection underneath tectonic plates (Yamato et al., 2013; Husson et al., 2015; Walker et al., 2016) and is most probably expressed through the widespread Neogene and Quaternary sequence of coastal landforms (marine terrace rasas) found along the shores of Western Europe.

6 Conclusion

On the Cotentin Peninsula, the typical coastal sequence culminates at ~200 m and includes up to four low-rising, clearly distinguished marine terraces overlooked by up to four rasas. Based on previous dating of the last interglacial maximum (MIS 5e) marine terrace in N Cotentin, as well as on modelling, we derived: 1) a mean Upper Pleistocene (MIS 5e) apparent uplift rate of 0.04 ± 0.01 mm/yr; 2) a mean "high" Middle Pleistocene eustasy-corrected of 0.09 ± 0.03 mm/yr and 3) a low constant uplift rate of 0.01 mm/yr using a synchronous correlation approach. Extrapolation of these rates reveals that the onset of the sequence of N Cotentin Peninsula started between ~ 3 Ma and ~ 15 Ma ago. The palaogeographic evolution of the Cotentin Peninsula (Normandy, France) corresponds to the emergence of rocky islands and islets that gradually merged together, and thereafter to the continent, ultimately forming a peninsula. Furthermore, through compilation of former data, we highlight that such morphostratigraphy - Pleistocene terraces overlooked by widespread Mio-

Pliocene rasas - is representative of Western Europe (except the British Isles) and, to a larger extent, is related to the generalized Cenozoic compression that accompanies the convergence between Africa and Eurasia.

Acknowledgments: We thank the ANR GiSeLE as well as the INSU programme Sulamer Hople for funding. This research is in memoriam of Jean Pierre Lautridou who has shown the coastal sequences of North Cotentin to many of us.

Figure Captions

Figure 1: Index map **A)** Location of the Cotentin Peninsula in W Europe **B)** Coastal sequences in Normandy and Northern Brittany. Stars represent sites where a sequence of coastal landforms (marine terraces, raised beaches) includes the MIS 5e benchmark (data from Pedoja et al., 2011, 2014, see Table 1 supplementary data). **C)** Location of Plio-Pleistocene basins on the Cotentin Peninsula. Extents of Plio-Pleistocene basins from Dugué (2003). **1** Larmor-Pleubian, **2** Brehat, **3** Binic, **4** Cesson, **5** Port Morvan, **6** Dahouet, **7** Piegu, **8** NE Saint Malo, **9** Hacqueville, **10** Hauteville - Annoville, **11**Chausey, **12** Jersey, **13** and **14** Guernsey SE and W. **15** le Rozel, **16** Alderney, **17** St Martin Jerd'heux, **18** Val de Saire, **19** Grandcamp Maisy, **20** St Côme - Asnelle - Meuvaine, **21** Graye, **22** le Havre. **Is** Island. **Ar** Archipelago. **LM** La Mondrée submerged terrace. **SV** Saint Sauveur le Vicomte. **SM** Sainteny

Marchésieux. Stars: coastal sequences including the MIS 5e landforms (Pedoja et al., 2011; 2014). Line: uplifted coastal stretch (Pedoja et al., 2014; this study).

Figure 2 : Idealized staircase coastal landscape. **A)** Sequence of marine terraces and rasas. **B)** Detail of a single marine terrace. **C)** Elevation transects.

Figure 3 : Extent of the high-resolution topography and results of the regional morphometric analysis. **A)** Shaded topography and high-roughness patches identified using the Surface Classification Model (SCM). **B-C)** results of surface classification model SCM. **D-E)** Example of SCM classification and mapping of marine terrace surfaces. **E-F**) Histograms of slope and roughness used to calibrate the SCM, selected ranges include 90% of the data.

Figure 4: The coastal sequences of the Cotentin Peninsula. **A)** Surface classification model displaying flat surfaces interpreted as sequences of marine terraces and rasas. **B - C)** Histogram of elevation v/s surface of SCM patches of N and S Cotentin. Levels are defined using elevation ranges, the width of each band represent the position of the outer and inner edge of marine terraces and rasas. **D)** Schematic mapping of North Cotentin marine terrace and rasas. **E) - F)** Swaths profiles across the Cotentin Peninsula, north and south, respectively.

Figure 5: Coastal sequence at Point and Cape de La Hague. **A)** General mapping **B)** Detailed mapping **C)** GPS Profile

Figure 6: Interpreted pictures of the sequence in N. Cotentin **A)** Low-standing T1 terrace at Goury **B)** Rasa and covered sequence of Ecalgrain Embayment **C)** Low-standing terrace at Anse de Vauville.

Figure 7: Morphometry of the rasa surfaces at La Hague Point. **A)** Surface classification model and swath profiles (black rectangles) used to map inner edges (black dots). **B)** Box plot of inner edge elevations for each rasa at both sides of La Hague Point. Dashed lines indicate the mean elevation. Notice that the difference between inner edges at both sides of the ridge is less than 2 m. **C)** Scatter plots of cliff height versus inner edge elevations of each rasa. Red line is a lineal regression and associated correlation coefficient (R^2), notice positive slope suggesting that these cliffs were formed by sea erosion (see text for further details).

Figure 8: Hypothesis on the timing of formation of the sequence from N Cotentin **A)** The sequence with dated terrace and elevations of the strandlines **B)** the short-

lasting hypothesis : Pliocene onset of the Cotentin coastal sequences **C)** the long-lasting hypothesis: Miocene onset of the Cotentin coastal sequences.

Figure 9: Synchronous correlation method applied to the four (T1 to T4) low-standing terraces in Cotentin. Methods as in Roberts et al., 2013. **A)** Predicted versus measured elevations of the shoreline angle of the low-standing marine terraces of N Cotentin **B)** Uplift rates and RMS deviation

Figure 10: Coastal uplift of Western Europe **A)** MIS 5e. The dotted line represent for the British Isles, the frontier between uplifting coasts (to the north) and subsiding coasts (to the south), for the period of time 0-6 ka as in Lambeck, (1991; 1996) and Shennan and Horton, (2002). see text for more details **B)** MIS 11 and MIS 7 isolated **C)** Old shorelines

Table 1: Mean Upper Pleistocene Coastal Uplift rates of N Cotentin

Table 2: Hypothesis on middle Pleistocene apparent and eustasy-corrected uplift rates of North Cotentin

Table 3: Hypothesis on the age of the upper rasas extrapolating various uplift rates

Table 4: Result of the synchronous method modelling, elevations in red indicate that younger sea-level high-stands would destroy the older high-stand shorelines or, in some cases, suggest that shorelines and their terraces may be caused by more than one sea-level high-stand.

References cited

Allard, M. and G. Tremblay (1981). "Observations sur le Quaternaire de l'extrémité orientale de la péninsule de Gaspé, Québec." Géographie physique et Quaternaire **35**(1): 105-125.

Alonso, A. and J. L. Pagés (2000). "El registro sedimentario del final del cuaternario en el litoral noroeste de la peninsula Iberica. Margenes Cantabrico y Atlantico." Revista de la Sociedad Geologica de España **13**(1): 17-29.

Alvarez-Marrón, J., R. Hetzel, S. Niedermann, R. Menéndez and J. Marquínez (2008). "Origin, structure and exposure history of a wave-cut platform more than 1 Ma in age at the coast of northern Spain: A multiple cosmogenic nuclide approach." Geomorphology **93**(3-4): 316-334.

Andersen, M. B., C. H. Stirling, E.-K. Potter, A. N. Halliday, S. G. Blake, M. T. McCulloch, B. F. Ayling and M. O'Leary (2008). "High-precision U-series measurements of more than 500,000 year old fossil corals." Earth and Planetary Science Letters **265**(1-2): 229-245.

Antoine, P., J.-P. Coutard, P. Gibbard, B. Hallegouet, J.-P. Lautridou and J.-C. Ozouf (2003). "The Pleistocene rivers of the English Channel region." Journal of Quaternary Science **18**(3-4): 227-243.

Antoine, P., J. P. Lautridou, J. Sommé, P. Auguste, J. P. Auffret, S. Baize, M. Clet-Pellerin, J.-P. Coutard, Y. Dewolf, O. Dugué, F. Joly, B. Laignel, M. Laurent, M. Lavollé, P. Munaut, P. Lebret, F. Lécolle, D. Lefebvre, N. Limondin-Lozouet, A.-V. Munaut, J.-C. Ozouf, F. Quesnel and D. Rousseau (1998). "Les formations quaternaires de la France du Nord-Ouest : Limites et corrélations [The quaternary formations of North-West France :." Quaternaire **9**(3): 227-241.

Arkell, W. J. (1943). "The Pleistocene rocks at trebetherick point, north Cornwall: their interpretation and correlation." Proceedings of the Geologist's Association **LIV**(part 4): 141-170.

Auffret, J.-P., D. Alduc, C. Larsonneur and A. J. Smith (1980). "Cartographie du réseau des paléovallées et de l'épaisseur des formations superficielles meubles de la Manche orientale." Annales de l'Institut Océanographique, Paris **58**(8): 21-35.

Authemayou, C., K. Pedoja, A. Heddar, S. Molliex, A. Boudiaf, B. Ghaleb, B. Vliet Lanoe, B. Delcaillau, H. Djellit, K. Yelles and M. Nexer (2017). "Coastal uplift west of Algiers (Algeria): pre- and post-Messinian sequences of marine terraces and rasas and their associated drainage pattern." International Journal of Earth Sciences: 1-23.

Baden-Powell, D. F. W. (1955). "The correlation of the Pliocene and Pleistocene marine beds of Britain and the Mediterranean." Proceedings of the Geologists' Association **66**(part 4): 271-292.

Baize, S. (1998). Tectonique, eustatisme et climat dans un systeme geomorphologique cotier. Le nord-ouest de la france au plio-pleistocene : exemple du cotentin (normandie). Géologie. Caen, University of Caen**:** 333 p.

Balescu, S., S. C. Packman, A. G. Wintle and R. Grün (1992). "Thermoluminescence dating of the middle Pleistocene raised beach of Sangatte (Northern France)." Quaternary Research **37**(3): 390-396.

Ballèvre, M., V. Bosse, C. Ducassou and P. Pitra (2009). "Palaeozoic history of the Armorican Massif: Models for the tectonic evolution of the suture zones." Comptes Rendus Geoscience **341**(2-3): 174-201.

Barrell, J. (1915). "Factors in movements of the strand line and theirs results in the Pleistocene and Post-Pleistocene." American Journal of Science Fourth Series **XL**(235): 1-22.

Bates, M. R., D. H. Keen and J. P. Lautridou (2003). "Pleistocene marine and periglacial deposits of the English Channel." Journal of Quaternary Science **18**(3-4): 319-337.

Battistini, R. and J. P. Bergoeing (1982). "Un exemple de côte à structure faillée quadrillée et néotectonique active : la côte pacifique du Costa Rica (The pacific coast of Costa Rica)." Bulletin de l'Association de géographes français **487-488**: 199-205.

Baudet, J.-L. (1959). "Les industries des plages suspendues (de 5m) du Nord de la France." Bulletin et Mémoires de la Société d'anthropologie de Paris **Xe série. Tome 10** (Fascicule 4): 285-301.

Bauer, H., P. Bessin, P. Saint-Marc, J.-J. Châteauneuf, C. Bourdillon, R. Wyns and F. o. Guillocheau (2016). "The Cenozoic history of the Armorican Massif: New insights from the deep CDB1 borehole (Rennes Basin, France)." Comptes Rendus Geoscience **348**(5): 387-397.

Benabdellouahed, M., O. Dugué, B. Tessier, I. Thinon and P. Guennoc (2013). "Evolution pléistocène de la Seine fluviatile préservée en Baie de Seine." Bulletin de l'Association Française pour l'Etude du Quaternaire **24**(3): 267-277.

Benedetti, M. M., J. A. Haws, C. L. Funk, J. M. Daniels, P. A. Hesp, N. F. Bicho, T. A. Minckley, B. B. Ellwood and S. L. Forman (2009). "Late Pleistocene raised beaches of coastal Estremadura, central Portugal." Quaternary Science

Reviews **28**(27-28): 3428-3447.

Bertotti, G. and M. Gouiza (2012). "Post-rift vertical movements and horizontal deformations in the eastern margin of the Central Atlantic: Middle Jurassic to Early Cretaceous evolution of Morocco." International Journal of Earth Sciences **101**(8): 2151-2165.

Bessin, P., F. Guillocheau, C. Robin, J.-M. Schroëtter and H. Bauer (2015). "Planation surfaces of the Armorican Massif (western France):Denudation chronology of a Mesozoic land surface twice exhumed in response to relative crustal movements between Iberia and Eurasia." Geomorphology **233**: 75-91.

Bigot, A. (1897). "Sur les dépôts pléistocènes et actuels du littoral de la Basse-Normandie." Comptes Rendus de l'Académie des Sciences, Paris **115**: 380.

Bigot, A. (1898). "Feuille des Pieux." Bulletin de la Carte Géologique **63**(Tome X): 1-7.

Bigot, A. (1930). "Les terrasses pléistocènes du littoral du Cotentin." Livre Jubilaire de la Société Géologique de France **tI**: 133-148.

Bigot, A. (1931). Les terrasses littorales du Cotentin. Congrès International de Géographie, Paris Librairie Armand Colin.

Bintanja, R. and R. S. W. Van de Wal (2008). "North American ice-sheet dynamics and the onset of 100,000-year glacial cycles." Nature **454**(7206): 869-872.

Bonnet, S., F. Guillocheau, J.-P. Brun and J. Van Den Driessche (2000). "Large scale relief development related to Quaternary tectonic uplift of a Proterozoic-Paleozoic basement: The Armorican Massif, NW France." Journal of Geophysical Research: Solid Earth **105**(B8): 19273-19288.

Bonow, J. M., P. Japsen, P. F. Green, P. R. Cobbold, A. J. Pedreira, R. Lilletveit and D. Chiossi (2009). "Post-rift landscape development of north-east Brazil." Geological Survey of Denmark and Greenland Bulletin **17**: 81-84.

Bowles, C. J. and E. Cowgill (2012). "Discovering marine terraces using airborne LiDAR along the Mendocino-Sonoma coast, northern California." Geosphere

8(2): 386-402.

Bradley, W. C. (1957). "Origin of marine terrace deposits in the Santa Cruz area, California." Bulletin of the Geological Society of America **68**: 421-444.

Bradley, W. C. and G. B. Griggs (1976). "Form, genesis, and deformation of central California wave-cut platforms." Geological Society of America bulletin **87**(3): 433-449.

Brault, N., S. Bourquin, F. Guillocheau, M. P. Dabard, S. Bonnet, P. Courville, J. Esteoule-Choux and F. Stepanoff (2004). "Mio-Pliocene to Pleistocene paleotopographic evolution of Brittany (France) from a sequence stratigraphic analysis: relative influence of tectonics and climate." Sedimentary Geology **163**(3): 175-210.

Breton, G., R. Cousin, M.-F. Huault, C. Lechevallier and D. Lefebvre (1991). "Les sédiments quaternaires du quartier de l'Hôtel de Ville, au Havre : séquences marines pré-éemienne, éemienne et holocène de l'estuaire de la Seine." Bulletin trimestrielle de la Société géologique de Normandie et amis du Muséum du Havre **78**(4): 15-63.

Breuil, H., M. Vaultier and G. Zbyszewski (1942). "Les Plages anciennes portugaises entre les Caps d'Espichel et Carvoeiro et leurs industries paléolithiques." Bulletin de la Société Préhistorique de France **Tome 39**(3-4): 93-98.

Bridgland, D. R. (2002). "Fluvial deposition on periodically emergent shelves in the Quaternary: example records from the shelf around Britain." Quaternary International **92**(1): 25-34.

Brodie, J. and N. White (1994). "Sedimentary basin inversion caused by igneous underplating: Northwest European continental shelf." Geology **22**(2): 147-150.

Bull, A. J. (1941). "Pleistocene chronology." Proceedings of the Geologists' Association **LIII**(part I): 1-44.

Burrough, P. A. and R. A. McDonnell (1998). "Creating continuous surfaces from point data." Principles of Geographic Information Systems. Oxford University Press, Oxford, UK.

Butaeye, D., E. Laville and J. Le Gall (2001). "Géomètrie et ciématique des chevauchements varisques du Nord-Est du Massif armoricain (France)." Comptes Rendus de l'Académie des Sciences - Series IIA - Earth and Planetary Science **332**(4): 283-289.

Campar de Almeida, A. (2001). "A carsificacao da serra da Boa Viagem: um processo Quaternario." Estudos do Quaternario Revista da Associaçao Portuguesa para o Estudo do Quaternario **4**: 29-33.

Caputo, R. (2007). "Sea-level curves: Perplexities of an end-user in morphotectonic applications." Global and Planetary Change **57**(3-4): 417-423.

Chambers, R. (1848). Ancient Sea-margins, as memorial of changes in the relative level of sea and land. Edinburgh, W & R Chambers.

Clet-Pellerin, M., S. Baize, A.-V. Walter, O. Dugué and J.-P. Coutard (1997). "Mise en évidence d'un interglaciaire du Pléistocène inférieur dans une formation fluviatile du Seuil du Cotentin (Normandie, France)." Géographie Physique et Quaternaire **51**(3): 363-378.

Cliquet, D. (2015). Les occupations néandertaliennes : des sites spécialisés (250 000 à 40 000 ans) Dans les pas de Néandertal : Les premiers hommes en Normandie de 500 000 à 5 000 ans avant notre ère. S. Berthelot, D. Cliquet and J.-M. Levesque. Caen, Faton Edition**:** 84-91.

Cliquet, D. and J. P. Lautridou (2009). "Les occupations humaines du Pléistocène moyen de Normandie dans leur cadre environnemental." Quaternaire **20**(3): 305-320.

Cliquet, D., J. P. Lautridou, M. Lamothe, N. Mercier, J.-L. Schwenninger, P. Alix and G. Vilgrain (2009). "Nouvelles données sur le site majeur d'Ecalgrain: Datations radiométriques et occupations humaines de la pointe de la Hague (Cotentin, Normandie)." Quaternaire **20**(3): 345-359.

Cliquet, D., N. Mercier, H. Valladas, L. Froget, D. Michel, B. Van Vliet-Lanoë and G. Vilgrain (2003). "Apport de la thermoluminescence sur silex chauffés à la chronologie de sites paléolithiques de Normandie : nouvelles données et interprétations " Quaternaire **14**(1): 51-64.

Coutard, J.-P. and J. P. Lautridou (1975). "Le Quaternaire de Grandcamp

(Calvados), Loess et plages marines normanniennes: un problème de datation." Bulletin de la Société Linnéenne de Normandie **104**(136-144).

Coutard, J.-P., J. P. Lautridou, D. Lefebvre and M. Clet (1979). "Les bas-niveaux marins éemien et pré-éemien de Grandcamp - les - bains." Bulletin de la Société Linneénne de Normandie **107**: 11-20.

Coutard, S. (2003). Formations quaternaires en bordure d'une mer épicontinentale, la Manche : tectonique, eustatisme, climat et occupations humaines. Exemple du Val de Saire (Normandie, France). Caen, Université de Caen**:** 445.

Coutard, S., J. P. Lautridou and E. Rhodes (2005). "Discontinuités dans l'enregistrement des cycles glaciaires interglaciaires sur un littoral en contexte intraplaque, exemple du Val de Saire (Normandie, France) " Quaternaire **16**(3): 217-227.

Coutard, S., J.-P. Lautridou, E. Rhodes and M. Clet (2006). "Tectonic, eustatic and climatic significance of raised beaches of Val de Saire, Cotentin, Normandy, France." Quaternary Science Reviews **25**(5-6): 595-611.

Cunha, L. S., A. A. Martins, J. Cabral, M. P. Gouveia, J.-P. Buylaert and A. S. Murray (2015). Staircases of wave-cut platforms in western central Portugal (Cape Mondego to Cape Espichel) - relevance as indicators of crustal uplift. VIII Simposio sobre el Margen Iberico Atlantico, Malaga Centro Oceanografico de Malaga.

Cunha, P. P., A. A. Martins, J. Cabral, M. P. Gouveia, J.-P. Buylaert and A. S. Murray (2015). Escadrias de terraços marinhos em Portugal centro-ocidental - relevância como indicadores de soerguimento crustal. VOO Congresso Nacional de Geomorfologia Lisboa

Daly, R. A. (1925). "Pleistocene changes of level." American Journal of Science - fifth serie **X**(58): 281-313

Davies, B. J., D. R. Bridgland, D. H. Roberts, C. O. Cofaigh, S. M. Pawley, I. Candy, B. Demarchi, K. E. H. Penkman and W. E. N. Austin (2009). "The age and stratigraphic context of the Easington Raised Beach, County Durham, UK." Proceedings of the Geologists' Association **120**(4): 183-198.

Dawson, A. G., S. Dawson, A. G. Cooper, A. Gemmell and R. Bates (2013). "A Pliocene age and origin for the strandflat of the Western Isles of Scotland: a speculative hypothesis." Geological Magazine **150**(02): 360-366.

Depéret, C. (1918-1922). "Essai de coordination chronologique générale des temps quaternaires : les formations marines " Extraits des Comptes rendus des séances de l'Académie des Sciences **166,480,636,884,167,418,979,168,868,873,170,159,171,212,174,1502,1594**.

Dèzes, P., S. M. Schmid and P. A. Ziegler (2004). "Evolution of the European Cenozoic Rift System: interaction of the Alpine and Pyrenean orogens with their foreland lithosphere." Tectonophysics **389**(1): 1-33.

Døssing, A., P. Japsen, A. B. Watts, T. Nielsen, W. Jokat, H. Thybo and T. Dahlae• Jensen (2016). "Miocene uplift of the NE Greenland margin linked to plate tectonics: Seismic evidence from the Greenland Fracture Zone, NE Atlantic." Tectonics **35** (2) : 257-282

Dugué, O. (2003). "The Pliocene to Early Pleistocene marine to fluviatile succession of the Seuil du Cotentin basins (Armorican Massif, Normandy, France)."

Journal of Quaternary Science **18**(3-4): 215-226.

Dugué, O., J.-P. Auffret and N. Poupinet (2007). "Cenozoic shelly sands in the Cotentin (Armorican Massif, Normandy, France): A record of Atlantic transgressions and intraplate Cenozoic deformations." Comptes Rendus Geoscience **339**(2): 110-120.

Dugué, O., J. P. Lautridou, F. Quesnel, M. Clet, N. Poupinet and C. Bourdillon (2009). "Évolution sédimentaire cénozoïque (Paléocène à Pléistocène inférieur) de la Normandie." Quaternaire **20**(3): 275-303.

Dunlop, A. (1893). "On Raised Beaches and Rolled Stones at High Levels in Jersey." Quarterly Journal of the Geological Society **49**(1-4): 523-530.

Dupret, L., E. Dissler, F. Doré, F. Gresselin and J. Le Gall (1990). "Cadomian geodynamic evolution of the northeastern Armorican Massif (Normandy and Maine)." Geological Society, London, Special Publications **51**(1): 115-131.

Dutton, A., E. Bard, F. Antonioli, T. M. Esat, K. Lambeck and M. T. McCulloch (2009).

"Phasing and amplitude of sea-level and climate change during the penultimate interglacial." Nature Geosciences **2**(5): 355-359.

Elhaï, H. (1960). "A propos des niveaux marins quaternaires en Normandie." Bulletin de la Société Linnéenne de Normandie **1**: 137-145.

Ferreira Soares, A. (1999). "As unidades Pliocenicas e Quaternarias no espaço do baixo Mondego (uma perspectiva de ordem)." Estudos do Quaternario Revista da Associaçao Portuguesa para o Estudo do Quaternario **2**: 7-17.

Ferreira Soares, A., P. M. Callapez and J. Fonseca Marques (2007). "The Farol deposit (deposito do Farol) - a pleistocene beach deposit from Cape Mondego (Figueira da Foz, West Central Portugal)." Ciencas da Terra (UNL) **16**: 163-173.

Figueiredo, P. M., J. Cabral and T. K. Rockwell (2011). Plio-Pleistocene tectonic activity in the Southwest of Portugal. 2nd INQUA - IGCP 567 International workshop on Active Tectonics, Earthquake Geology, Archealogy and engineering, Corinth, Greece.

Fleury, L., J.-P. Clément, F. o. Ménillet, G. Moguedet, C. Vinchon and G. Farjanel (1989). "Les sables rouges et graviers des plateaux et des karsts du Maine méridional; Etude sédimentologique." Géologie de la France **1**(2): 255-257.

Font, M., J.-L. Lagarde, D. Amorese, J.-P. Coutard and J.-C. Ozouf (2002). "Une méthode de quantification de la dégradation d'un escarpement de faille au cours des cycles climatiques du Quaternaire : la faille de Jobourg (Nord Cotentin, France)." Comptes Rendus Geoscience **334**(3): 171-178.

Frankel, K. L. and J. F. Dolan (2007). "Characterizing arid region alluvial fan surface roughness with airborne laser swath mapping digital topographic data." Journal of Geophysical Research: Earth Surface **112**(F2).

Garcin, M., G. Farjanel, S. Courbouleix, P. Barrier, P. Braccini, G. Brébion, R. P. Carbonel, J. C. Carriol and M. Clet-Pellerin (1997). "La longue séquence Pliocène de Marchésieux -résultats analytiques et premiers résultats " Géologie de la France **3**: 39-77.

Gautier, M. (1967). "La tectonique tertiaire dans le massif Armoricain." Annales de Géographie **414**: 168-197.

Gibbard, P.L. (1988). "The history of the great northwest European rivers during the past three million years". Philosophical Transactions of the Royal Society of London, Series B **318:** 559-602

Gonzalez-Acebron, L., R. Mas, J. Arribas, J. M. Gutierrez-Mas and C. Perez-Garrido (2016). "Very coarse-grained beaches as a response to generalized sea level drops in a complex active tectonic setting: Pleistocene marine terraces at the Cadiz coast, SW Spain." Marine Geology **382**(Supplement C): 92-110.

Graindor, M. J. (1964). "Le Quaternaire marin de Normandie." Bulletin de la Société Géologique de Normandie et des Amis du Muséum du Havre **54**: 1-15.

Grant, K. M., E. J. Rohling, C. B. Ramsey, H. Cheng, R. L. Edwards, F. Florindo, D. Heslop, F. Marra, A. P. Roberts and M. E. Tamisiea (2014). "Sea-level variability over five glacial cycles." Nature communications **5**(5076).

Green, P. F., I. R. Duddy, P. Japsen, J. M. Bonow and J. A. Malan (2016). "Post-breakup burial and exhumation of the southern margin of Africa." Basin Research. **29** (1): 96-127

Gresselin, F. (2000). Evolution varisque du Massif armoricain oriental : insertion dans une transversale ouest-européenne. Ecole de Géologie Structurale Caen, University of Caen**:** 335 p.

Guilcher, A. (1949). "Aspects et problèmes morphologiques du massif de Devon-Cornwall comparés à ceux d'Armorique." Revue de Géographie Alpine **37**(4): 689-717.

Guilcher, A. (1951). "La formation de la mer du Nord, du Pas-de-Calais et des plaines maritimes environnantes." Revue de géographie de Lyon **26**(3): 311-329.

Guilcher, A. (1969). "Pleistocene and Holocene sea level changes " Earth Sciences Review **5**: 69-97.

Guilcher, A. (1974). "Les «rasas» : un problème de morphologie littorale générale." Annales de Géographie **83**(455): 1-33.

Guilcher, A. and B. Hallegouet (1981). "Le haut cordon de galets Pléistocène de Ruvein en Plovan (Finistère) et ses enseignements généraux." Bulletin de l'Association Française pour l'Etude du Quaternaire **18**(6): 75-82.

Guillocheau, F., N. Brault, E. Thomas, J. Barbarand, S. Bonnet, S. Bourquin, J. Estéoule-Choux, P. Guennoc, D. Menier, D. Néraudeau, J.-N. Proust and R. Wyns (2003). "Histoire géologique du Massif Armoricain depuis 140 Ma (Crétacé-Actuel)." Bulletin Information Géologique du Bassin de Paris **40**(1): 13-28.

Hallégouët, B. (1976). "Les anciens dépôts marins et fluviatiles de la vallée de l'Elorn (Finistère) " Norois **89**: 55-72.

Hamblin, R.J.O. Crosby, A. Balson, P.S. Jones, S.M. Chadwick, R.A., Penn I.E., Arthur M.J. (1992). The Geology of the English Channel. United Kingdom Offshore Regional Report, British Geological Survey. HMSO: London; 106 pp

Home, H. (1912). "Worked flints obtained from the 25-foot raised beach near Holywood, co. Down." Nature **2248**(90): 361.

Husson, L., P. Yamato and A. Bézos (2015). "Ultraslow, slow, or fast spreading ridges: Arm wrestling between mantle convection and far-field tectonics." Earth and Planetary Science Letters **429**: 205-215.

Japsen, P., J. Bonow, P. Green, J. Chalmers and K. Lidmar- Bergström (2006). "Elevated, passive continental margins: Long-term highs or Neogene uplifts? New evidence from West Greenland." Earth and Planetary Science Letters **248**: 330-339.

Japsen, P., J. M. Bonow, P. F. Green, P. R. Cobbold, D. Chiossi, R. Lilletveit, L. P. Magnavita and A. Pedreira (2012). "Episodic burial and exhumation in NE Brazil after opening of the South Atlantic." Geological Society of America Bulletin **124**(5-6): 800-816.

Japsen, P. and J. A. Chalmers (2000). "Neogene uplift and tectonics around the

North Atlantic: overview." Global and Planetary Change **24**(3): 165-173.

Jara-Muñoz, J. and D. Melnick (2015). "Unraveling sea-level variations and tectonic uplift in wave-built marine terraces, Santa Maria Island, Chile." Quaternary Research **83**(1): 216-228.

Jara-Muñoz, J., D. Melnick and M. R. Strecker (2016). "TerraceM: A MATLAB® tool to analyze marine and lacustrine terraces using high-resolution topography." Geosphere **12**(1): 176-195.

Jara-Muñoz J, Melnick D, Zambrano P, Rietbrock A, Gonzáles J, Argandoña B, Strecker MR. (2017): "Quantifying offshore forearc deformation and splay-fault slip using drowned Pleistocene shorelines, Arauco Bay, Chile". Journal of Geophysical Research, Solid Earth, **122** (6) 4529–4558.

Jardine, W. G. (1981). "The determination of former shoreline positions in areas of large tidal range, with examples taken mainly from Scotland." Bulletin de l'Association française pour l'étude du quaternaire **18**(2): 67-70.

Juignet, P. (1980). "Transgressions-régressions, variations eustatiques et influences tectoniques de l'Aptien au Maastrichtien dans le Bassin de Paris occidental et sur la bordure du Massif armoricain." Cretaceous Research **1**(4): 341-357.

Klein (1975). "Massif armoricain et Bassin parisien." Fondation Baulig **Vol 2**

Kopp, R. E., F. J. Simons, J. X. Mitrovica, A. C. Maloof and M. Oppenheimer (2009). "Probabilistic assessment of sea level during the last interglacial stage." Nature **462**(7275): 863-867.

Lagarde, J. L., D. Amorese, M. Font, E. Laville and O. Dugué (2003). "The structural evolution of the English Channel area." Journal of Quaternary Science **18**(3-4): 201-213.

Lagarde, J.-L., S. Baize, D. Amorese, B. Delcaillau, M. Font and P. Volant (2000). "Active tectonics, seismicity and geomorphology with special reference to Normandy (France)." Journal of Quaternary Science **15**(7): 745-758.

Lajoie, K. R. (1986). Coastal Tectonics. Active tectonic. N. A. Press. Washington

D,C, National Academic Press**:** 95-124.

Lajoie, K. R., D. J. Ponti, C. L. Powell, A. M. Mathieson and A. M. Sarna - Wojcicki (1991). Emergent marine strandlines and associated sediments, coastal California: a record of Quaternary sea-level fluctuations, vertical tectonic movements, climatic changes, and coastal processes. Quaternary Nonglacial Geology: Conterminous U.S.: The Geology of North America. Morrison. Boulder, Colorado, Geological Society of America. **K-2:** 190-214.

Lambeck, K. (1991). "Glacial rebound and sea-level change in the British Isles." Terra Nova **3**(4): 379-389.

Lambeck, K. (1996). "Glaciation and sea-level change for Ireland and the Irish Sea since Late Devensian/Midlandian time." Journal of the Geological Society **153**(6): 853-872.

Larsonneur, C., R. Horn, J. P. Auffret, P. Hommeril and A. Moal (1975). "Geologie de la Partie Meridionale de la Manche Centrale." Philosophical Transactions of the Royal Society of London A: Mathematical, Physical and Engineering Sciences **279**(1288): 145-153.

Lautridou, J. P. (1983). Le Quaternaire de Normandie. Caen, Centre de Géomorphologie du CNRS.

Lautridou, J. P. (1985). Le cycle périgaciaire pléistocène en Europe du Nord-Ouest et plus particulièrement en Normandie. Centre de Géomorphologie du CNRS. Caen, University of Caen. **Doctorat d'état:** 970.

Lautridou, J. P. (1989). "Les lignes de rivages Pléistocènes en Normandie âge des plates-formes littorales." Bulletin du Centre de Géomorphologie du CNRS, Caen **36**: 231-234.

Lautridou, J. P., S. Baize, M. Clet, J.-P. Coutard and J.-C. Ozouf (1999). "Les séquences plio-pléistocènes littorales et estuariennes de Normandie." Quaternaire **10**(2-3): 161-169.

Leorri, E., F. Fatela, T. Drago, S. L. Bradley, J. Moreno and A. Cearreta (2012). "Lateglacial and holocene coastal evolution of the Minho estuary (N Portugal) : implications for understanding sea-level changes in Atlantic Iberia." The

Holocene **23**(3): 353-363.

Lericolais, G., J.-P. Auffret and J.-F. Bourillet (2003). "The Quaternary Channel River: seismic stratigraphy of its palaeo-valleys and deeps." Journal of Quaternary Science **18**(3-4): 245-260.

Lisiecki, L. E. and M. E. Raymo (2005). "A Pliocene-Pleistocene stack of 57 globally distributed benthic delta 18 O records." Paleoceanography **20**: PA1003.

Lyell, C. (1830). Principles of geology, being an attempt to explain the former changes of the earth's surface, by reference to causes now in operation. London, John Murray.

Mellett, C. L., D. M. Hodgson, A. J. Plater, B. Mauz, I. Selby and A. Lang (2013). "Denudation of the continental shelf between Britain and France at the glacialâ€“interglacial timescale." Geomorphology **203**: 79-96.

Melnick, D. (2016). "Rise of the central Andean coast by earthquakes straddling the Moho." Nature Geoscience.**9**: 401-416.

Miller, K. G., M. A. Kominz, J. V. Browning, J. D. Wright, G. S. Mountain, M. E. Katz, P. J. Sugarman, B. S. Cramer, N. Christie-Blick and S. F. Pekar (2005). "The Phanerozoic record of global sea-level change." science **310**(5752): 1293-1298.

Milne, G. A., A. J. Long and S. E. Bassett (2005). "Modelling Holocene relative sea-level observations from the Caribbean and South America." Quaternary Science Reviews **24**(10-11): 1183-1202.

Moore, D. (1842). "On fossil bones found on the surface of a raised beach at the Hoe, near Plymouth." Transactions of the Geological Society **IV**(3rd series): 97-98.

Moreno, F. and J. Mediato (2009). Terrazas del rio Miera. Difluencia durante su desarollo (Cantabria). 6 Simposio sobre el Margen Iberico Atlantico, Oviedo

Murray-Wallace, C. and C. Woodroffe (2014). Quaternary sea level : a global perspective. Cambridge, Cambridge University Press.

Nexer, M. (2015). Etudes conjointe des réseaux de drainage et des paléocôtes plio-quaternaires soulevées:exemples de l'Indonésie et du Golfe Normand Breton. Caen, University of Caen. **PhD:** 374 pp

Oliva (1977). "La plateforme Moghrébienne : néotectonique et eustatisme sur le littoral de l'Anti-Atlas." Méditerranée **Deuxième série, Tome 29**(2): 73-91.

Pareyn, C. (1980). "Mise en évidence d'une activité néotectonique pliocène et quaternaire dans le Cotentin, le bassin de Carentan et le Bessin (Manche et Calvados)." Bulletin de la Société Géologique de France **tome XXII**(4): 695-701.

Paskoff, R. and P. Sanlaville (1983). "Les côtes de la Tunisie, variations du niveau marin depuis le tyrrhénien. Travail réalisé dans le cadre de l'ERA 345 du CNRS " Collection de la Maison de l'Orient Méditerranéen : Série Géographique et Préhistorique: 190.

Pedoja, K., J. F. Dumont, M. Lamothe, L. Ortlieb, J.-Y. Collot, B. Ghaleb, M. Auclair, V. Alvarez and B. Labrousse (2006) a. "Plio-Quaternary uplift of the Manta Peninsula and La Plata Island and the subduction of the Carnegie Ridge, central coast of Ecuador." Journal of South American Earth Sciences **22**(1-2): 1-21.

Pedoja, K., L. Ortlieb, J. F. Dumont, M. Lamothe, B. Ghaleb, M. Auclair and B. Labrousse (2006) b. "Quaternary coastal uplift along the Talara Arc (Ecuador, Northern Peru) from new marine terrace data." Marine Geology **228**(1-4): 73-91.

Pedoja, K., L. Husson, V. Regard, P. R. Cobbold, E. Ostanciaux, M. E. Johnson, S. Kershaw, M. Saillard, J. Martinod, L. Furgerot, P. Weill and B. Delcaillau (2011). "Relative sea-level fall since the last interglacial stage: Are coasts uplifting worldwide?" Earth-Science Reviews **108**(1-2): 1-15.

Pedoja, K., L. Husson, M. E. Johnson, D. Melnick, C. Witt, S. Pochat, M. Nexer, B. Delcaillau, T. Pinegina, Y. Poprawski, C. Authemayou, M. Elliot, V. Regard and F. Garestier (2014). "Coastal staircase sequences reflecting sea-level oscillations and tectonic uplift during the Quaternary and Neogene." Earth-Science Reviews **132**(0): 13-38.

Pellerin, J., P. Brebion, M. Helluin, J.-T. Hollin, A. Lauriat - Rage, D. Lefévre and G. H. Miller (1987). "Données nouvelles sur le gisement marin Quaternaire +

14.5/15.7 m NGF du cimetière de Luc sur mer (Calvados, France)." Bulletin du Centre de Géomorphologie du CNRS, Caen **32**(99-115).

Pellerin, J. and P. A. Dupeuble (1979). "Le bas niveau marin Eemien de Graye-sur-Mer (Calvados)." Bulletin Société Linnéene de Normandie **107**: 21-26.

Peulvast, J.-P., V. C. Sales, F. o. Bâtard and Y. Gunnell (2008). "Low post-Cenomanian denudation depths across the Brazilian Northeast: implications for long-term landscape evolution at a transform continental margin." Global and Planetary Change **62**(1): 39-60.

Prestwich, J. (1851). "On the Drift at Sangatte Cliff, near Calais." Quarterly Journal of the Geological Society **7**(1-2): 274-278.

Prestwich, J. (1862-1863). "Theoretical considerations on the condition under which the drift deposits containing the remains of extinct mammalia and flint-implements were accumulated : and on their geological age." Proceedings of the Royal Society of London **12**: 38-52.

Prestwich, J. (1865). "Additional Observations on the Raised Beach of Sangatte with reference to the Date of the English Channel, and the Presence of Loess in the Cliff Section." Quarterly Journal of the Geological Society **21**(1-2): 440-442.

Prestwich, J. (1892). "The Raised Beaches, and 'Head' or Rubble-drift, of the South of England: their Relation to the Valley Drifts and to the Glacial Period; and on a late post-Glacial Submergence." Quarterly Journal of the Geological Society **48**(1-4): 263-343.

Quezada, J., G. Gonzalez, T. Dunai, A. Jensen and J. Juez-Larré (2007). "Alzamiento litoral Pleistoceno del norte de Chile: edades 21Ne de la terraza costera más alta del área deCaldera-Bahía Inglesa." Revista Geológica de Chile **34**(1): 81-96.

Ramos, A. M. and P. P. Cunha (2009). O Pliocenico e o Plistocenico da plataforma litoral entre os paralelos da Serra da Boa Viagem e da Nazaré (Portugal central). 6e simposio sobre a margem iberico atlantica, Oviedo.

Ramos, A. M., P. P. Cunha, L. S. Cunha, A. Gomes, F. C. Lopes, J.-P. Buylaert and

A. S. Murray (2012). "The River Mondego terraces at the Figueira da Foz coastal area (western central Portugal): geomorphological and sedimentological characterization of a terrace staircase affected by differential uplift and glacio eustasy " Geomorphology **165-166**: 107-123.

Ramos, A. M., P. P. Cunha, A. Gomes and L. S. Cunha (2010). Caracterizaçao geomorfologica e sedimentologica da escadaria de terraços da margem direita do rio Mondego, no sector entre Maiorca e Vila Verde. VI Seminario Latino Americano de Geografia Fisica II Seminario Ibero Americano de Geografia Fisica Coimbra, Universidad de Coimbra.

Raynal, J.-P., D. Lefevre, D. Geraads and M. El Graoui (1999). "Contribution du site paléontologique de Lissasfa (Casablanca, Maroc) à une nouvelle interprétation du Mio-Pliocène de la Méseta." Comptes Rendus de l'Académie des Sciences-Series IIA-Earth and Planetary Science **329**(8): 617-622.

Regard, V., M. Saillard, J. Martinod, L. Audin, S. Carretier, K. Pedoja, R. Riquelme, P. Paredes and G. Hérail (2010). "Renewed uplift of the Central Andes Forearc revealed by coastal evolution during the Quaternary." Earth and Planetary Science Letters **297**(1-2): 199-210.

Regnauld, H., B. Mauz and M.-T. Morzadec-Kerfourn (2003). "The last interglacial shoreline in northern Brittany, western France." Marine Geology **194**(1-2): 65-77.

Renouf, J. and L. James (2011). "High level shore features of Jersey (Channel Islands) and adjacent areas." Quaternary International **231**(1-2): 62-77.

Roberts, G. P., M. Meschis, S. Houghton, C. Underwood and R. M. Briant (2013). "The implications of revised Quaternary palaeoshoreline chronologies for the rates of active extension and uplift in the upper plate of subduction zones." Quaternary Science Reviews **78**: 169-187.

Rohling, E. J., G. L. Foster, K. M. Grant, G. Marino, A. P. Roberts, M. E. Tamisiea and F. Williams (2014). "Sea-level and deep-sea-temperature variability over the past 5.3 million years." Nature **508**(7497): 477-482.

Rohling, E. J., K. Grant, M. Bolshaw, A. P. Roberts, M. Siddall, C. Hemleben and M. Kucera (2009). "Antarctic temperature and global sea level closely coupled over the past five glacial cycles." Nature Geosciences **2**: 500-504.

Rosenbaum, G., G. S. Lister and C. Duboz (2002). "Relative motions of Africa, Iberia and Europe during Alpine orogeny." Tectonophysics **359**(1-2): 117-129.

Sanlaville, P. (1974). "Le rôle de la mer dans les aplanissements côtiers du Liban." Revue de géographie de Lyon **49**(4): 295-310.

Scuvée, F. and D. Alduc (1981). "Deux niveaux marins Pléistocènes et leurs industries paléolithiques respectives sur le littoral du Cotentin (Manche)." Bulletin de la Société préhistorique française **tome 78**: 210-218.

Shakun, J. D., D. W. Lea, L. E. Lisiecki and M. E. Raymo (2015). "An 800-kyr record of global surface ocean Î´18O and implications for ice volume-temperature coupling." Earth and Planetary Science Letters **426**: 58-68.

Shennan, I. and B. Horton (2002). "Holocene land- and sea-• level changes in Great Britain." Journal of Quaternary science **17**(5-6): 511-526.

Sheppard, G. (1927). "Geological observations on Isla de la Plata, Ecuador, South America." American Journal of Science **13**: 480-486.

Sheppard, G. (1930). "The geology of southwestern Ecuador." American Association of Petroleum Geologist Bulletin **14**: 263-309.

Siddall, M., J. Chappell and E.-K. Potter (2006). Eustatic sea level during past interglacials. The Climate of Past Interglacials. F. Sirocko, M. Claussen, M. F. Sanchez Goñi and T. Litt. Amsterdam, Elsevier**:** 75-92.

Siddall, M., E. J. Rohling, A. Almogi-Labin, C. Hemleben, D. Meischner, I. Schmelzer and D. A. Smeed (2003). "Sea-level fluctuations during the last glacial cycle." Nature **423**(6942): 853-858.

Silva, C., B. Landau, R. Domènech and J. Martinelli (2010). "Pliocene Atlantic molluscan assemblages from the Mondego Basin (Portugal):age and palaeoceanographic implications." Palaeogeography, Palaeoclimatology, Palaeoecology **285**: 248-254.

Sommé, J. and P. Antoine (1989). "La plaine maritime de la mer du Nord (France) et le pas de Calais : du Pléistocène moyen à l'Holocène." Bulletin du Centre de Géomorphologie du CNRS, Caen **36**: 219-222.

Sommé, J., P. Antoine, N. Cunat-Bogé, D. Lefèvre and A. V. Munaut (1999). "The marine middle pleistocene of the north sea in France : Sangatte cliff and Herzeele formation." Quaternaire **10**(2-3): 151-160.

Spratt, R. M. and L. E. Lisiecki (2016). "A Late Pleistocene sea level stack." Climate of the Past **12**(4): 1079.

Stirling, C. H., T. M. Esat, K. Lambeck and M. T. McCulloch (1998). "Timing and duration of the Last Interglacial: evidence for a restricted interval of widespread coral reef growth." Earth and Planetary Science Letters **160**(3-4): 745-762.

Stirling, C. H., T. M. Esat, K. Lambeck, M. T. McCulloch, S. G. Blake, D.-C. Lee and A. N. Halliday (2001). "Orbital Forcing of the Marine Isotope Stage 9

Interglacial." Science **291**(5502): 290-293.

Sutcliffe, A. J., A. P. Currant and C. B. Stringer (1987). "Evidence of sea-level change from coastal caves with raised beach deposits, terrestrial faunas and dated stalagmites." Progress in oceanography **18**(1-4): 243-271.

Szabo, B. J. and J. G. Vedder (1971). "Uranium-series dating of some pleistocene marine deposits in southern California." Earth and Planetary Science Letters **11**: 283-290.

Teixeira, C. (1944). "Tectonica Plio-Pleistonica do Noroeste Peninsular." Boletim da Sociedade Geológica de Portugal **Vol. IV**(Fasc. I-II): 19-40.

Teixeira, C. (1948). "Les dépôts modernes du littoral portugais au Nord de Leiria." Boletim da Sociedade Geológica de Portugal **Vol. VII**(Fasc. I-II): 83-94.

Telfer, M., J. L. Schwenninger, R. T. Walker, R. A. Sloan, A. B. Watts, R. L. Kahle, B. Kahle and M. W. Dee (2016). "Rapid mantle-driven uplift along the Angolan margin in the late Quaternary." Nature Geoscience **9**: 909-914.

Tessier, B., N. Delsinne and P. Sorrel (2013). "Holocene sedimentary infilling of a tide-dominated estuarine mouth. The example of the macrotidal Seine estuary (NW France)." Bulletin de la Societe Geologique de France **181**(2): 87-98.

Texier, J.-P. and J. Meireles (1987). "As formaçoes Quaternarias do Litoral do Minho (Portugal): propostas para uma nova abordagem climato-cronologica e dinâmica." Cadernos de Arqueologia **Serie II**(4): 9-33.

Thompson, W. G. and S. L. Goldstein (2005). "Open-system coral ages reveal persistent suborbital sea-level cycles." Science **308**(5720): 401-404.

Thompson, W. G., M. W. Spiegelman, S. L. Goldstein and R. C. Speed (2003). "An open-system model for U-series age determinations of fossil corals." Earth and Planetary Science Letters **210**(1-2): 365-381.

van de Plassche, O. (1986). Sea-level research : a manual for the collection and evaluation of data. Norwich, UK, Geo Books.

van Vliet-Lanoë, B., M. Laurent, J. L. Bahain, S. Balescu, C. Falguères, M. Field, B. Hallégouët and D. H. Keen (2000). "Middle Pleistocene raised beach anomalies in the English Channel: regional and global stratigraphic implications." Journal of Geodynamics **29**(1-2): 15-41.

van Vliet-Lanoë, B., N. Vandenberghe, M. Laurent, B. Laignel, A. Lauriat-Rage, S. Louwye, J.-L. Mansy, D. Mercier, B. Hallegouet, F. Meilliez, Y. Michel, G. Moguedet and J.-P. Vidier (2002). "Palaeogeographic evolution of northwestern Europe during the Upper Cenozoic." Geodiversitas **24**(3): 511-541.

Vérague, J. (1983). "Le gisement sablo-graveleux cénozoïque probable du hameau du Cloquant (La Glacerie, Normandie)." Norois **118**: 293-302.

Waelbroeck, C., L. D. Labeyrie, E. Michel, J. C. Duplessy, J. F. McManus, K. Lambeck, E. Balbon and M. Labracherie (2002). "Sea-level and deep water temperature changes derived from benthic foraminefera isotopic records." Quaternary Science Reviews **21**: 295-305.

Westaway, R. (1993). "Quaternary uplift of Southern Italy." Journal of Geophysical

Research **98**(B12): 21 741-21 772.

Westaway, R. (2009). "Quaternary uplift of northern England." Global and Planetary Change **68**: 357-382.

Whittow, J. B. (1960). "Some comments on the raised beach platform of South West Caernarvonshire and on an unrecorded raised beach at Porth Neigwl, North Wales." Proceedings of the Geologist's Association **71**: 31-39.

Wythe Cooke, C. (1930). "Correlation of coastal terraces." The Journal of Geology **XXXVIII**(7): 577-589.

Yamato, P., L. Husson, T. W. Becker and K. Pedoja (2013). "Passive margins getting squeezed in the mantle convection vice." Tectonics **32**(6): 2013TC003375.

Yildirim, C., D. Melnick, P. Ballato, T. F. Schildgen, H. Echtler, A. E. Erginal, N. G. n. Käyak and M. R. Strecker (2013). "Differential uplift along the northern margin of the Central Anatolian Plateau: inferences from marine terraces." Quaternary Science Reviews **81**(0): 12-28.

Zachos, J. C., G. R. Dickens and R. E. Zeebe (2008). "An early Cenozoic perspective on greenhouse warming and carbon-cycle dynamics." Nature **451**(7176): 279-283.

Zazo, C., P. G. Silva, J. L. Goy, C. Hillaire Marcel, B. Ghaleb, J. Lario, T. Bardaji and A. Gonzalez (1999). "Coastal uplift in continental collision plate boundaries: data from the last interglacial marine terrace of the Gibraltar Strait area (South Spain)." Tectonophysics **301**: 95-109.

Ziegler, P. A. and P. Dèzes (2007). "Cenozoic uplift of Variscan Massifs in the Alpine foreland: Timing and controlling mechanisms." Global and Planetary Change **58**(1-4): 237-269.

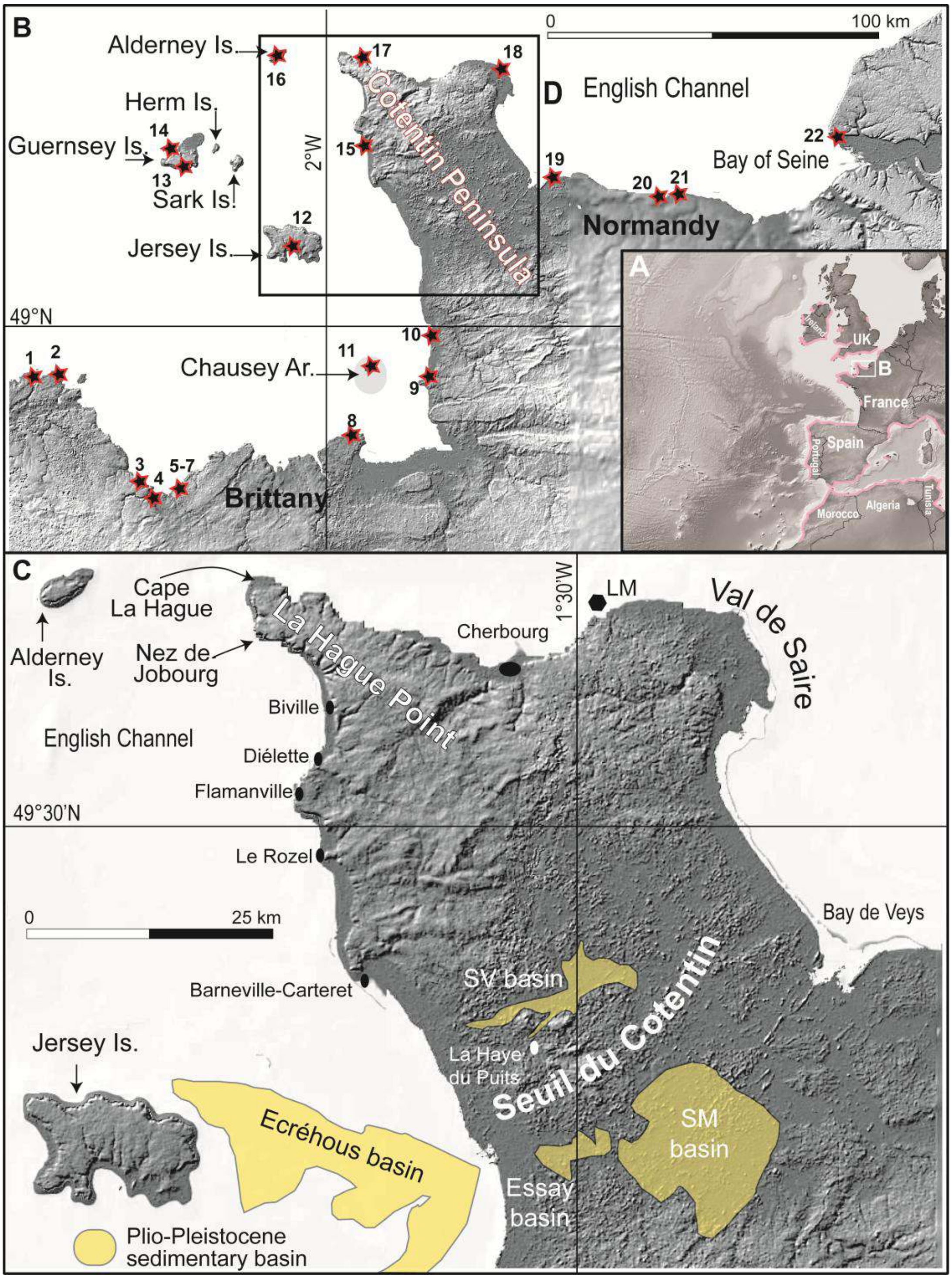
B
Alderney Is.
16
17
18
Herm Is.
Guernsey Is.
14
13
Sark Is.
2°W
15
Cotentin Peninsula
12
Jersey Is.
0
100 km
D
English Channel
22
Bay of Seine
19
20
21
Normandy
49°N
1
2
Chausey Ar.
11
10
9
8
3
4
5-7
Brittany
A
UK
B
France
Spain
Portugal
Morocco
Algeria
Tunisia
C
Cape La Hague
Alderney Is.
Nez de Jobourg
La Hague Point
1°30'W
LM
Cherbourg
Val de Saire
Biville
English Channel
Diélette
Flamanville
49°30'N
Le Rozel
0
25 km
Bay de Veys
SV basin
Barneville-Carteret
Seuil du Cotentin
Jersey Is.
La Haye du Puits
SM basin
Ecréhous basin
Essay basin
Plio-Pleistocene sedimentary basin

Figure 1

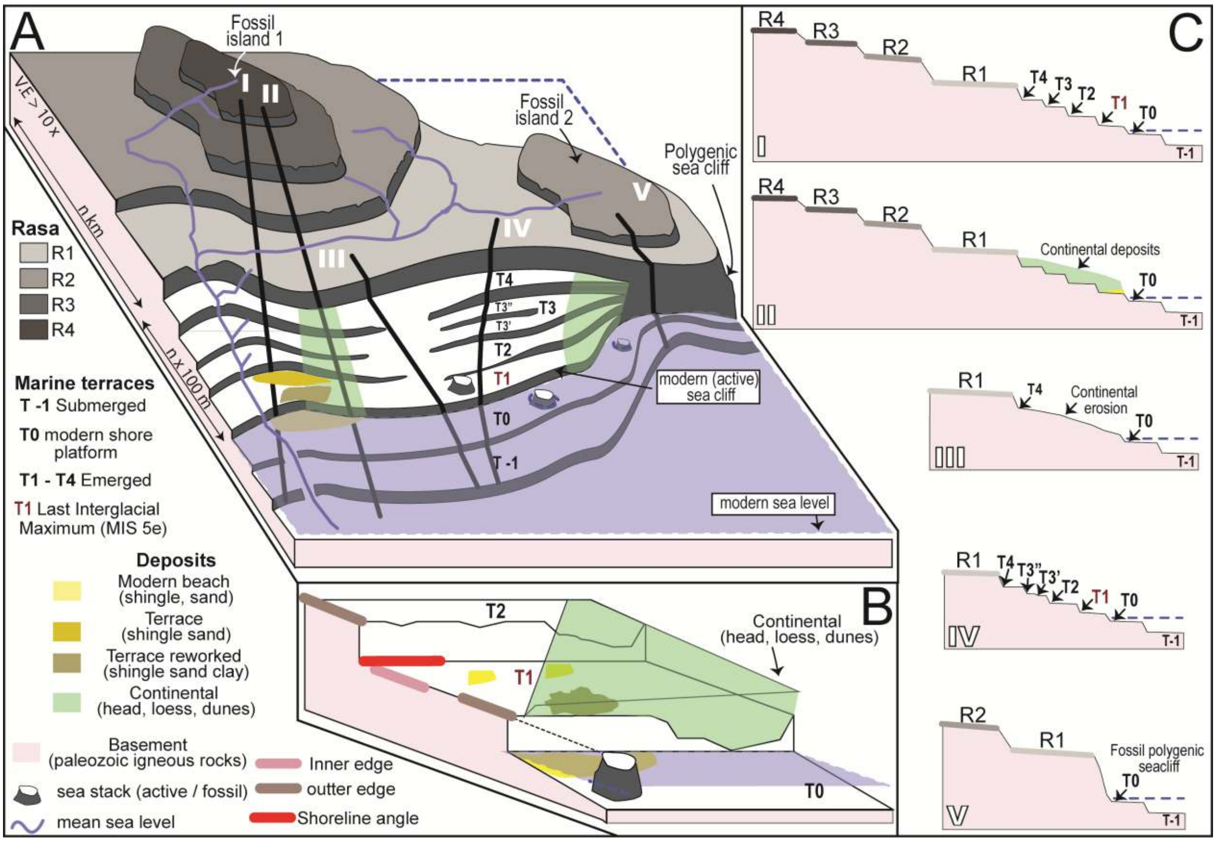
A
Fossil island 1
I
II
Fossil island 2
V
Polygenic sea cliff
V.E.> 10 x
n km
n x 100 m
III
IV
T4
T3"
T3'
T3
T2
T1
T0
T -1
modern (active) sea cliff
modern sea level
Rasa
R1
R2
R3
R4
Marine terraces
T -1 Submerged
T0 modern shore platform
T1 - T4 Emerged
T1 Last Interglacial Maximum (MIS 5e)
Deposits
Modern beach (shingle, sand)
Terrace (shingle sand)
Terrace reworked (shingle sand clay)
Continental (head, loess, dunes)
Basement (paleozoic igneous rocks)
sea stack (active / fossil)
mean sea level
Inner edge
outter edge
Shoreline angle
B
T2
T1
Continental (head, loess, dunes)
T0
C
R4
R3
R2
R1
T4
T3
T2
T1
T0
T-1
Continental deposits
Continental erosion
T3"
T3'
Fossil polygenic seacliff

Figure 2

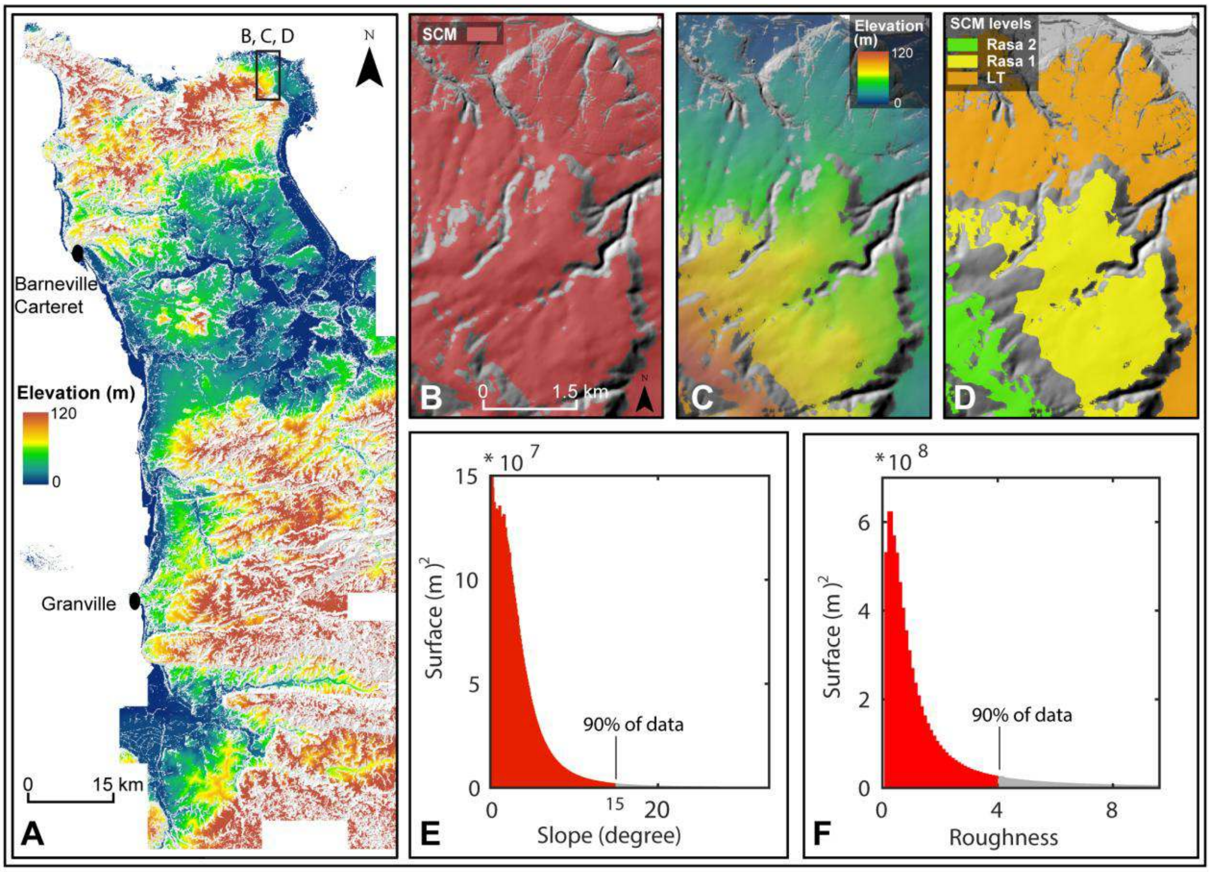

B, C, D
N
Barneville
Carteret
Elevation (m)
120
0
Granville
0
15 km
A
SCM
B
0
1.5 km
Elevation (m)
120
0
C
SCM levels
Rasa 2
Rasa 1
LT
D
* 10 7
15
10
5
0
Surface (m)2
90% of data
0
15
20
Slope (degree)
E
*10 8
6
4
2
0
Surface (m)2
90% of data
0
4
8
Roughness
F

Figure 3

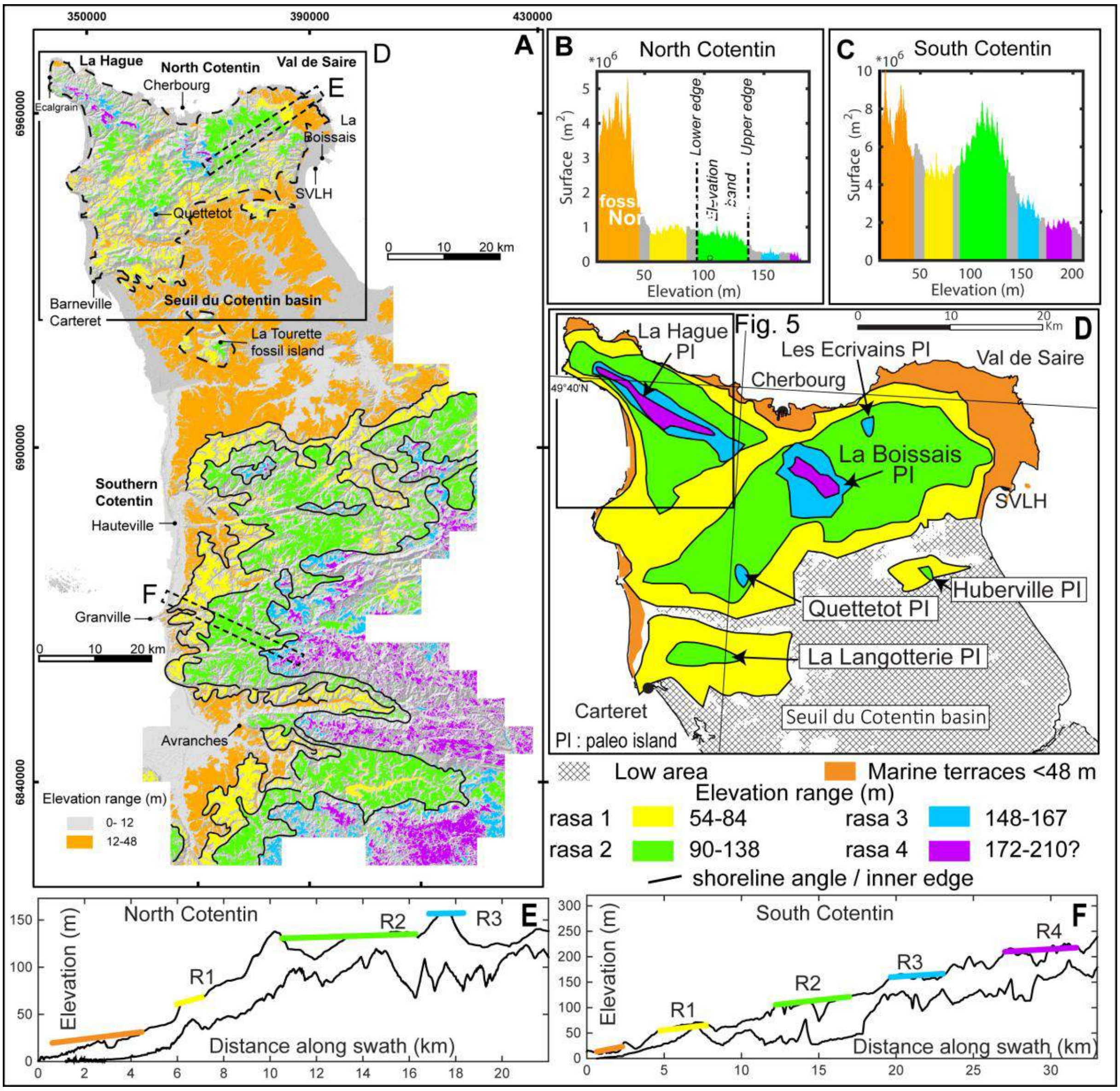

A
B
North Cotentin
C
South Cotentin
D
E
F
La Hague
North Cotentin
Val de Saire
Cherbourg
Ecalgrain
La Boissais
SVLH
Quettetot
Barneville Carteret
Seuil du Cotentin basin
La Tourette fossil island
Southern Cotentin
Hauteville
Granville
Avranches
Elevation range (m)
0- 12
12-48
Surface (m2)
Elevation (m)
Lower edge
Upper edge
La Hague PI
Les Ecrivains PI
La Boissais PI
Quettetot PI
Huberville PI
La Langotterie PI
Carteret
PI : paleo island
Fig. 5
49°40'N
Low area
Marine terraces <48 m
rasa 1 54-84
rasa 2 90-138
rasa 3 148-167
rasa 4 172-210?
shoreline angle / inner edge
R1
R2
R3
R4
Distance along swath (km)

Figure 4

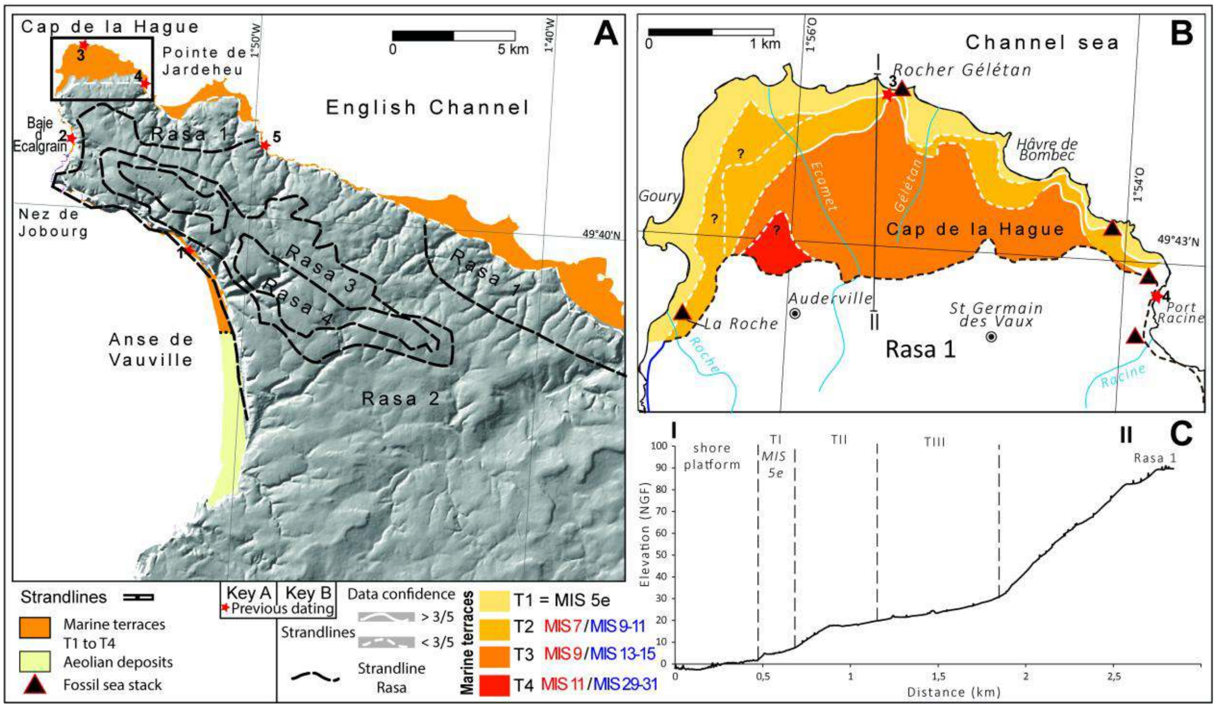
Cap de la Hague
Pointe de Jardeheu
English Channel
A
Baie d'Ecalgrain
Nez de Jobourg
Anse de Vauville
Rasa 1
Rasa 2
Rasa 3
Rasa 4
Channel sea
B
Rocher Gélétan
Hâvre de Bombec
Goury
Cap de la Hague
Auderville
La Roche
St Germain des Vaux
Port Racine
Rasa 1
C
shore platform
TI MIS 5e
TII
TIII
Elevation (NGF)
Distance (km)
Strandlines
Marine terraces T1 to T4
Aeolian deposits
Fossil sea stack
Key A
Key B
Previous dating
Data confidence
Strandlines
> 3/5
< 3/5
Strandline Rasa
Marine terraces
T1 = MIS 5e
T2 MIS 7 / MIS 9-11
T3 MIS 9 / MIS 13-15
T4 MIS 11 / MIS 29-31

Figure 5

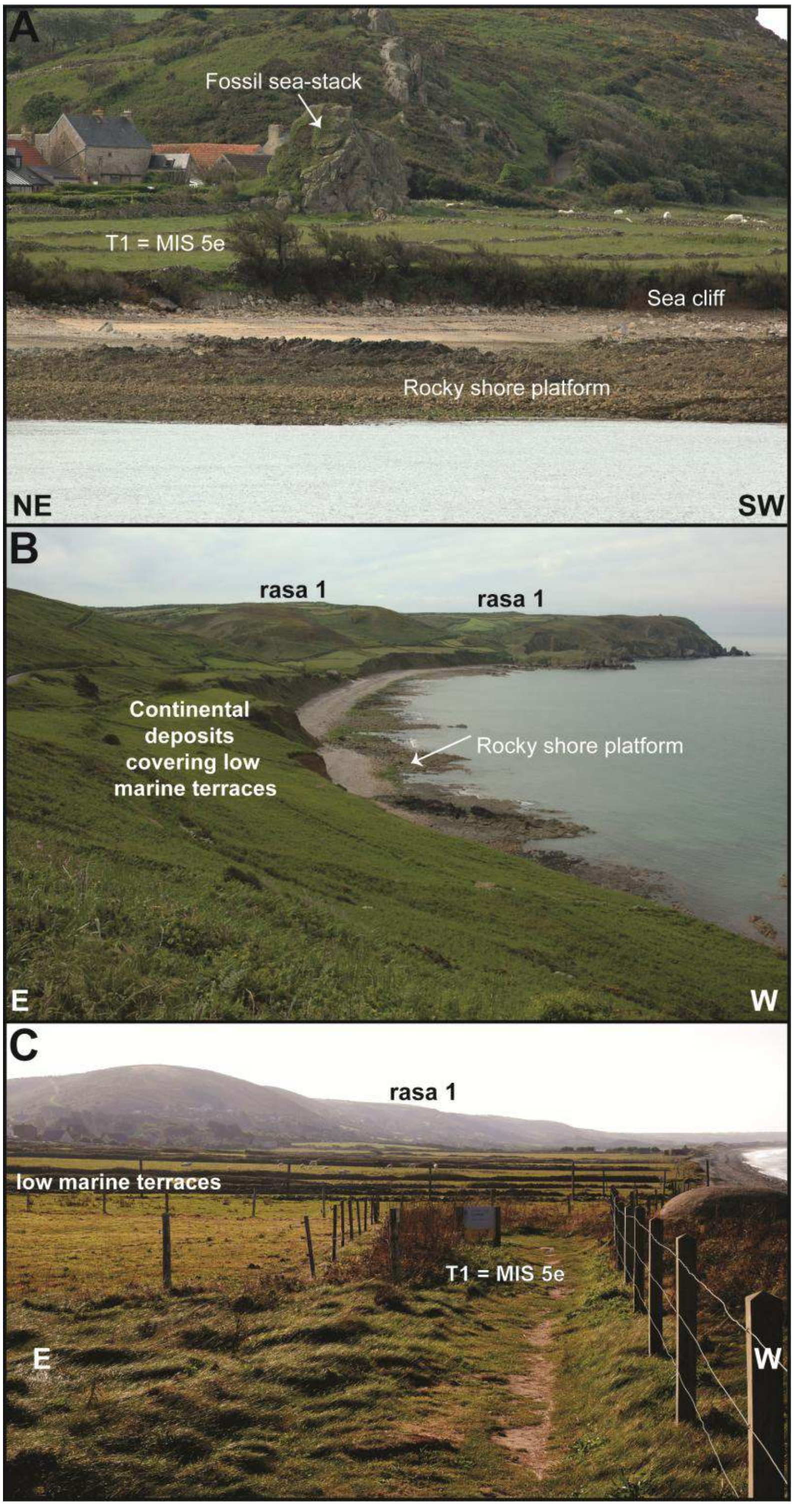
A
Fossil sea-stack
T1 = MIS 5e
Sea cliff
Rocky shore platform
NE
SW
B
rasa 1
rasa 1
Continental deposits covering low marine terraces
Rocky shore platform
E
W
C
rasa 1
low marine terraces
T1 = MIS 5e
E
W

Figure 6

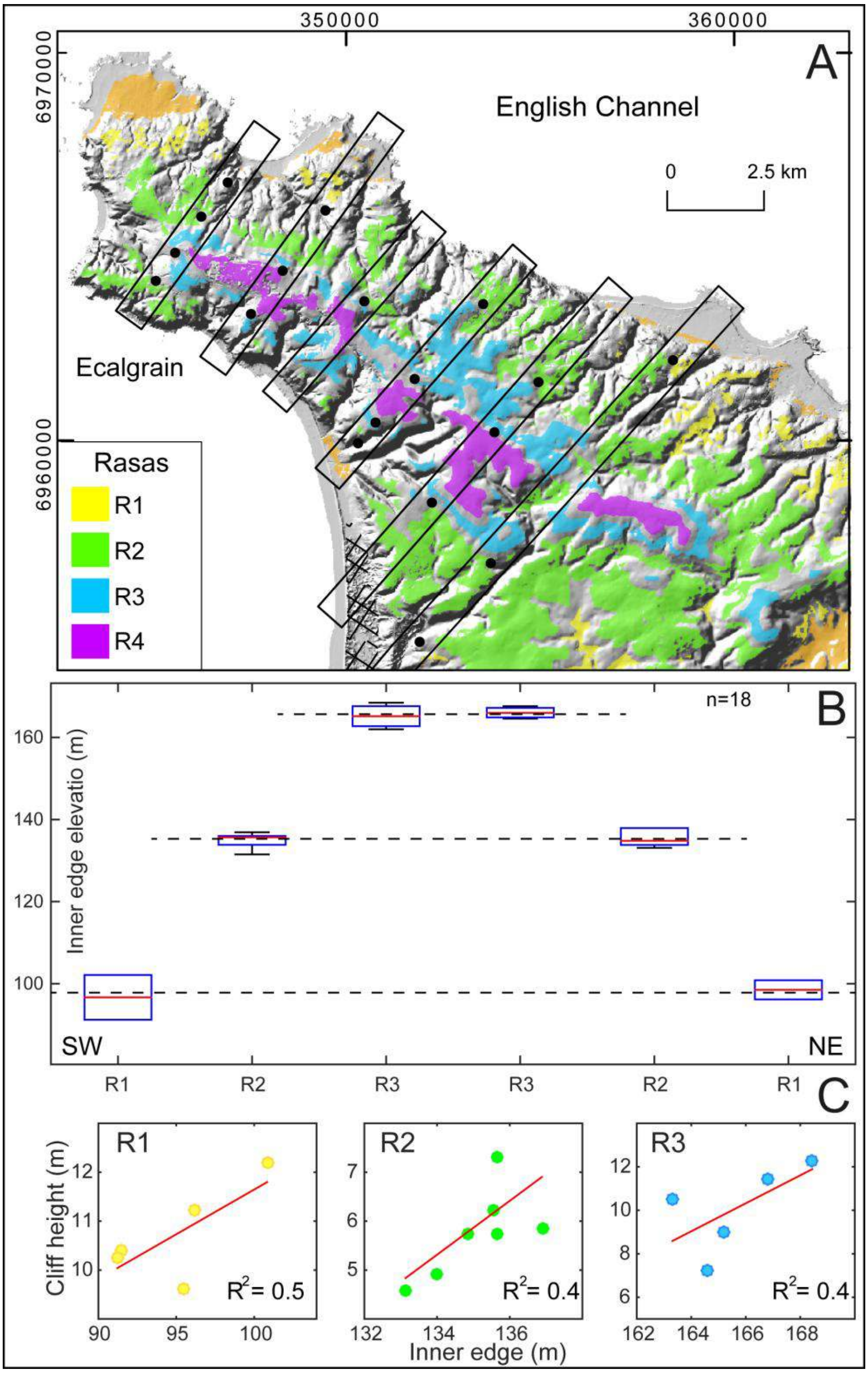

350000
360000
6970000
6960000
A
English Channel
0
2.5 km
Ecalgrain
Rasas
R1
R2
R3
R4
B
n=18
Inner edge elevatio (m)
160
140
120
100
SW
NE
R1
R2
R3
R3
R2
R1
C
R1
R2
R3
Cliff height (m)
12
11
10
R^2= 0.5
90
95
100
7
6
5
R^2= 0.4
132
134
136
Inner edge (m)
12
10
8
6
R^2= 0.4
162
164
166
168

Figure 7

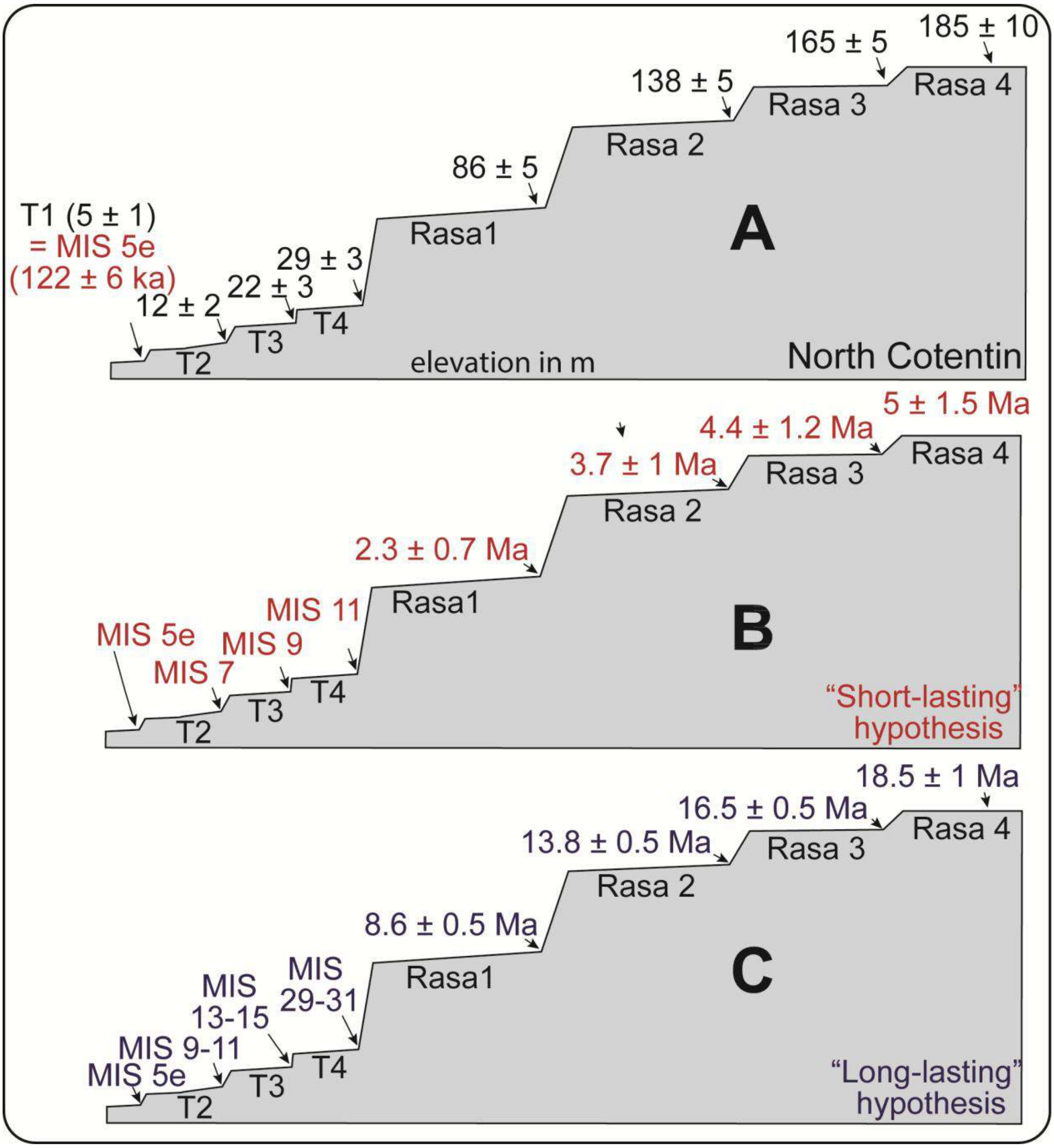

185 ± 10
165 ± 5
138 ± 5
Rasa 4
Rasa 3
Rasa 2
86 ± 5
Rasa1
T1 (5 ± 1)
= MIS 5e
(122 ± 6 ka)
29 ± 3
22 ± 3
12 ± 2
T4
T3
T2
A
elevation in m
North Cotentin
5 ± 1.5 Ma
4.4 ± 1.2 Ma
3.7 ± 1 Ma
Rasa 4
Rasa 3
Rasa 2
2.3 ± 0.7 Ma
Rasa1
MIS 11
MIS 9
MIS 7
MIS 5e
T4
T3
T2
B
"Short-lasting"
hypothesis
18.5 ± 1 Ma
16.5 ± 0.5 Ma
13.8 ± 0.5 Ma
Rasa 4
Rasa 3
Rasa 2
8.6 ± 0.5 Ma
Rasa1
MIS
29-31
MIS
13-15
MIS 9-11
MIS 5e
T4
T3
T2
C
"Long-lasting"
hypothesis

Figure 8

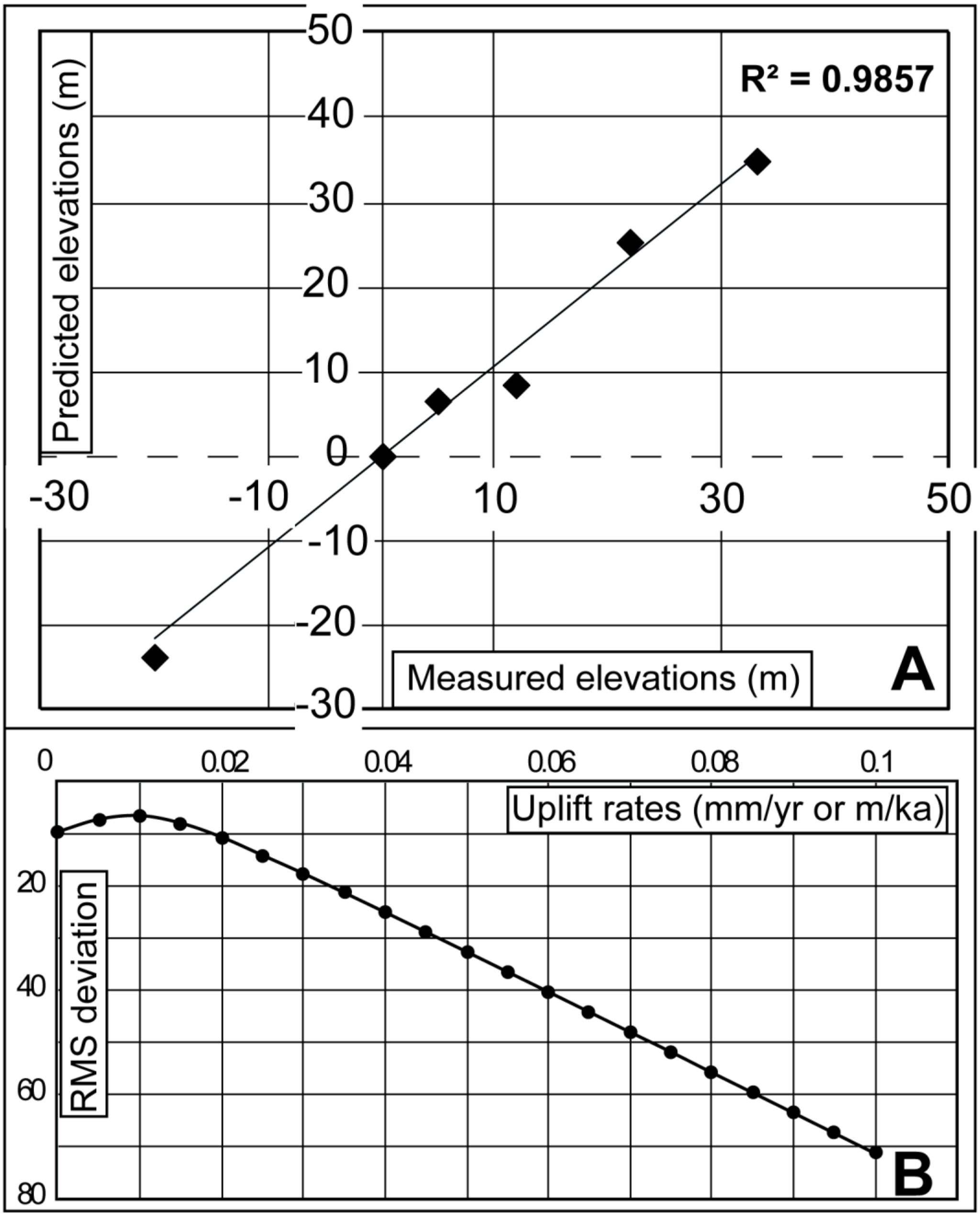

R² = 0.9857
Predicted elevations (m)
Measured elevations (m)
50
40
30
20
10
0
-10
-20
-30
-30
-10
10
30
50
A
0
0.02
0.04
0.06
0.08
0.1
Uplift rates (mm/yr or m/ka)
RMS deviation
20
40
60
80
B

Figure 9

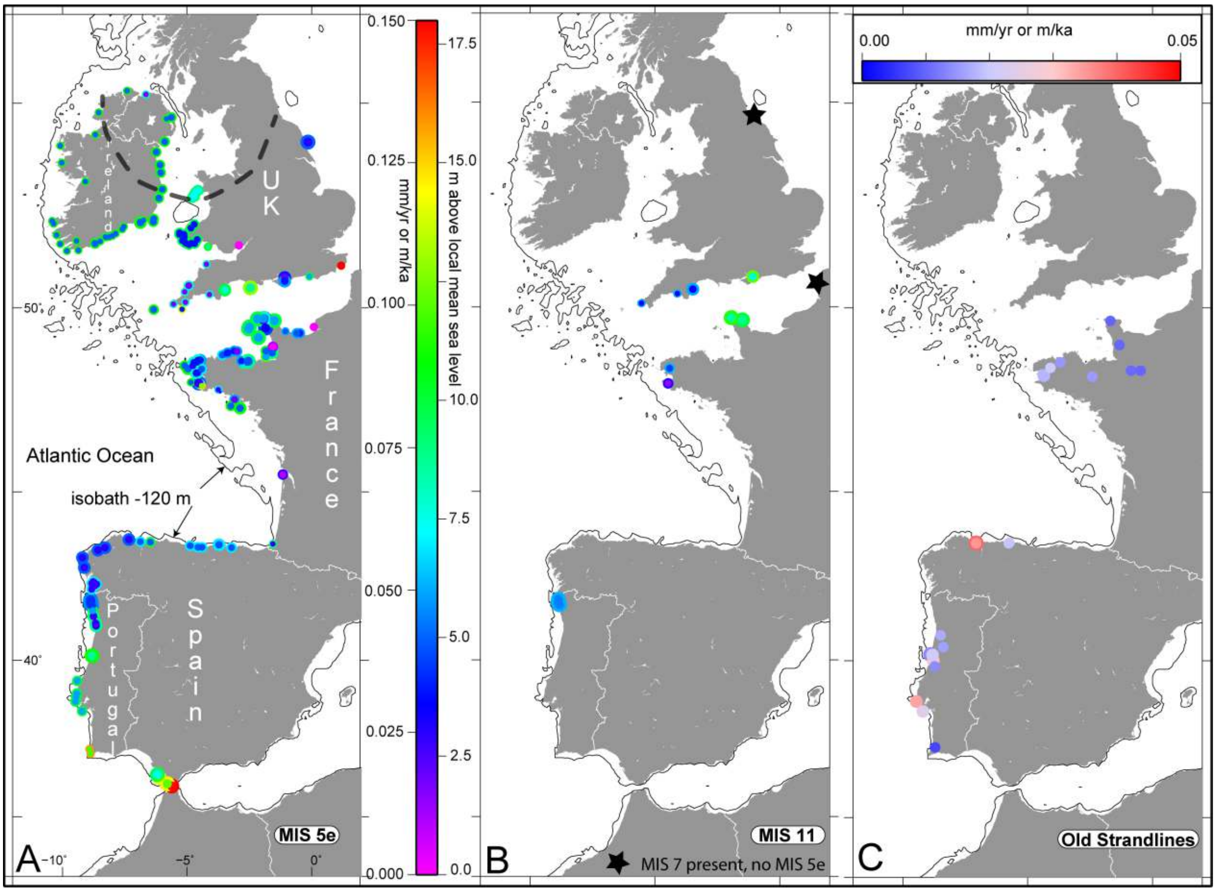

Ireland
UK
France
Portugal
Spain
Atlantic Ocean
isobath -120 m
MIS 5e
A
-10°
-5°
0°
50°
40°
0.150
0.125
0.100
0.075
0.050
0.025
0.000
mm/yr or m/ka
17.5
15.0
10.0
7.5
5.0
2.5
0.0
m above local mean sea level
B
MIS 11
MIS 7 present, no MIS 5e
C
mm/yr or m/ka
0.00
0.05
Old Strandlines

Figure 10

Area	Site	Terrace	Chrono-stratigraphy	Dating Method	Reference	Elevations						Age MIS		Apparent uplift rates				Eustatic correction Murray-Wallace and Woodroffe (2014)		Corrected Uplift rate Murray-Wallace and Woodroffe (2014)				Eustatic correction Waelbroeck et al. (2002)	
						Elevation of deposits / Landfor		Elevation Strandline / NGF		Elevation Strandline / landform															
						Ed	MoE	Es	MoE	Es	MoE	age	MoE	U max	U min	U mean	MoE	e	MoE	U max	U min	U mean	MoE	e	MoE
East	Anse du Brick, Fermanville - Port Levy, Anse de Quéry	T1	MIS 5e	5 OSL dating	Coutard, 2003; Coutard et al., 2005; 2006	*	*	7	1	**5**	**1**	122	6	0.05	0.03	0.04	0.01	6	4	0.03	-0.05	-0.01	0.04	6	13
West	Herquemoulin	T1	MIS 5e	Palynology	Clet, 1983	2	1	7	1	**5**	**1**	122	6	0.05	0.03	0.04	0.01	6	4	0.03	-0.05	-0.01	0.04	6	13
	Cap de la Hague	T1	MIS 5e	morphostratigraphy	this study	*	*	7	1	**5**	**1**	122	6	0.05	0.03	0.04	0.01	6	4	0.03	-0.05	-0.01	0.04	6	13

Site	Corrected Uplift rate Waelbroeck et al. (2002)				Eustatic correction Bintanja and Van der Wal (2008)		Corrected Uplift rate Bintanja and Van der Wal (2008)				Eustatic correction Grant et al. (2014)		Corrected Uplift rate Grant et al. (2014)				Eustatic correction Shakun et al. (2015)		Corrected Uplift rate Shakun et al. (2015)				Eustatic correction Spratt and Lisiecki (2016)			Corrected Uplift rate Spratt and Lisiecki (2016)			
	U max	U min	U mean	MoE	e	MoE	U max	U min	U mean	MoE	e	MoE	U max	U min	U mean	MoE	e	MoE	U max	U min	U mean	MoE	e	Moe (+)	MoE (-)	U max	U min	U mean	MoE
Anse du Brick, Fermanville - Port Levy, Anse de Quéry	0.11	-0.12	0.00	0.11	0	8	0.12	-0.03	0.04	0.08	5	14	0.13	-0.12	0.01	0.12	-10	10	0.22	0.03	0.13	0.10	3	12	20	0.13	-0.13	0.00	0.13
Herquemoulin	0.11	-0.12	0.00	0.11	0	8	0.12	-0.03	0.04	0.08	5	14	0.13	-0.12	0.01	0.12	-10	10	0.22	0.03	0.13	0.10	3	12	20	0.13	-0.13	0.00	0.13
Cap de la Hague	0.11	-0.12	0.00	0.11	0	8	0.12	-0.03	0.04	0.08	5	14	0.13	-0.12	0.01	0.12	-10	10	0.22	0.03	0.13	0.10	3	12	20	0.13	-0.13	0.00	0.13

Table 1

Terrace	Chrono-stratigraphy	Elevation Strandine / NGF		Elevation Strandline / landform		Age MIS		Apparent uplift rates landform			
		Es	MoE	Es	MoE	age	MoE	U max	U min	U mean	MoE
T1	MIS 5e	7	1	**5**	**1**	122	6	0.05	0.03	**0.04**	**0.01**
T2	MIS 7	15	2	**12**	**2**	217.5	27.5	0.07	0.04	**0.06**	**0.02**
T3	MIS 9	25	3	**22**	**3**	324.5	18.5	0.08	0.06	**0.07**	**0.01**
T4	MIS 11	33	3	**29**	**3**	390	30	0.09	0.06	**0.08**	**0.01**
										0.06	**0.01**

Terrace	Eustatic correction Murray-Wallace and Woodroffe (2014)		Corrected Uplift rate Murray-Wallace and Woodroffe (2014)				Eustatic correction Waelbroeck et al. (2002)		Corrected Uplift rate Waelbroeck et al. (2002)			
	e	MoE	U max	U min	U mean	MoE	e	MoE	U max	U min	U mean	MoE
T1	6	4	0.03	-0.05	**-0.01**	**0.04**	6	13	0.11	-0.12	**0.00**	**0.11**
T2	-8	12	0.18	0.02	**0.10**	**0.08**	-4	13	0.16	0.00	**0.08**	**0.08**
T3	3	2	0.08	0.04	**0.06**	**0.02**	5	13	0.11	0.00	**0.06**	**0.05**
T4	9.5	3.5	0.07	0.03	**0.05**	**0.02**	6	13	0.11	0.02	**0.06**	**0.05**
					0.05	**0.04**					**0.05**	**0.07**

Terrace	Eustatic correction Bintanja and Van der Wal (2008)		Corrected Uplift rate Bintanja and Van der Wal (2008)				Eustatic correction Grant et al. (2014)			Corrected Uplift rate Grant et al. (2014)			
	e	MoE	U max	U min	U mean	MoE	e	Moe (+)	MoE (-)	U max	U min	U mean	MoE
T1	0	8	0.12	-0.03	**0.04**	**0.08**	5	14	14	0.13	-0.12	**0.01**	**0.12**
T2	-18	8	0.21	0.08	**0.15**	**0.06**	-12	21	28	0.28	0.00	**0.14**	**0.14**
T3	0	8	0.11	0.03	**0.07**	**0.04**	-10	10	15	0.16	0.06	**0.11**	**0.05**
T4	0	8	0.11	0.04	**0.08**	**0.03**	-6	10	15	0.15	0.05	**0.10**	**0.05**
					0.08	**0.05**						**0.09**	**0.09**

Terrace	Eustatic correction Shakun et al. (2015)		Corrected Uplift rate Shakun et al. (2015)				Eustatic correction Spratt and Lisiecki (2016)			Corrected Uplift rate Spratt and Lisiecki (2016)			
	e	MoE	U max	U min	U mean	MoE	e	Moe (+)	MoE (-)	U max	U min	U mean	MoE
T1	-10	10	0.22	-0.03	**0.10**	**0.13**	3	12	20	0.20	-0.09	**0.06**	**0.14**
T2	-16	16	0.24	-0.01	**0.12**	**0.13**	-7	18	24	0.24	0.00	**0.12**	**0.12**
T3	-27	18	0.23	0.02	**0.12**	**0.10**	3	15	30	0.17	0.00	**0.09**	**0.08**
T4	-5	23	0.17	0.02	**0.09**	**0.07**	3	17	28	0.16	0.01	**0.09**	**0.07**
					0.11	**0.11**						**0.09**	**0.10**

Table 2

		Elevation		Apparent MIS 5e uplift rates				Corrected Middle Pleistocene uplift rates				Corrected upper Pleistocene uplift rates			
				U maximum	U minimum	U mean		U maximum	U minimum	U mean		U maximum	U minimum	U mean	
				0.05	0.03	0.04		0.12	0.06			0.01	0.01	0.01	
		E	**Moe**	**minimum extrapolated age**	**maximum extrapolated age**	**mean extrapolated age**	**mean extrapolated age error**	**minimum extrapolated age**	**maximum extrapolated age**	**mean extrapolated age**	**mean extrapolated age error**	**minimum extrapolated age**	**maximum extrapolated age**	**mean extrapolated age**	**mean extrapolated age error**
rasa 1	distal	54	5	980	1967	1473	493	408	983	696	288	4900	5900	5400	500
	proximal	**86**	**5**	**1620**	**3033**	**2327**	**707**	**675**	**1517**	**1096**	**421**	**8100**	**9100**	**8600**	**500**
rasa 2	distal	95	5	1800	3333	2567	767	750	1667	1208	458	9000	10000	9500	500
	proximal	**138**	**5**	**2660**	**4767**	**3713**	**1053**	**1108**	**2383**	**1746**	**638**	**13300**	**14300**	**13800**	**500**
rasa 3	distal	148	5	2860	5100	3980	1120	1192	2550	1871	679	14300	15300	14800	500
	proximal	**165**	**5**	**3200**	**5667**	**4433**	**1233**	**1333**	**2833**	**2083**	**750**	**16000**	**17000**	**16500**	**500**
rasa 4	distal	172	5	3340	5900	4620	1280	1392	2950	2171	779	16700	17700	17200	500
	proximal	**185**	**10**	**3500**	**6500**	**5000**	**1500**	**1458**	**3250**	**2354**	**896**	**17500**	**19500**	**18500**	**1000**

Table 3

MIS	Uplift rate (mm/yr)	Highstand (ka)	sea level corrected to to (m)	calculated expected IE (m)	Measured IE (m)	Terrace allocation
5c	**0.01**	**100**	**-25**	**-24**	**-20**	**offshore**
5e	**0.01**	**125**	**5**	**6**	**5**	**T1**
6d	0.01	175	-30	-28		
7a	0.01	200	-5	-3		
7c	0.01	217	-30	-28		
7e	0.01	240	-5	-3		
9a	0.01	285	-30	-27		
9c	0.01	310	-22	-19		
9e	**0.01**	**340**	**5**	**8**	**12**	**T2**
11c	0.01	410	-5	-1		
13a	0.01	478	0	6		
13c	**0.01**	**525**	**20**	**25**	**22**	**T3**
15a (?)	0.01	550	10	16		
15a (?)	0.01	560	3	9		
15c	0.01	590	20	26		
15e	0.01	620	20	26		
17c	0.01	695	10	17		
?	0.01	740	5	12		
19c?	0.01	800	20	28		
21a?	0.01	855	20	29		
?	**0.01**	**980**	**25**	**35**	**33**	**T4**

Table 4

Highlights

Morpho-stratigraphy of low-lying terraces from N Cotentin

Description of the polygenic coastal erosion surfaces (rasas) of Cotentin

Late Cenozoic paleogeographic evolution

Database on Neogene and Quaternary shorelines of Western Europe

Wholesale analysis of the Late Cenozoic uplift of Western European coastlines